MONODISPERSE POLYMERIC MICROPARTICLES AS ARTIFICIAL ANTIGEN PRESENTING CELLS FOR CANCER IMMUNOTHERAPY

by
Hongzhe Yu

A thesis submitted to Johns Hopkins University in conformity with the requirements for the degree of Master of Science in Engineering

Baltimore, Maryland
July, 2020

Abstract

Improved standardization and robustness of particle-based therapies is required to translate promising new biotechnologies to the clinic. In particular, more precise control over particle size, monodispersity, and batch-to-batch homogeneity are needed. A microfluidic technology was developed to enable polymeric microparticle synthesis with a narrow size distribution and improved control over particle sizes. Key parameters including microfluidic channel size, polymer solvent, polymer concentration, and microfluidic flow rates were independently investigated and characterized. By engineering these parameters in particle synthesis, monodisperse polymeric microparticles with tunable sizes were successfully produced. To demonstrate the utility of these monodisperse polymeric particles for use as a therapeutic, next-generation biomimetic artificial antigen presenting cells (aAPCs) were fabricated. Monodisperse PLGA microparticles were first synthesized in the new microfluidic devices and then functionalized with proteins to create aAPCs. Microfluidic preparation of the microparticles enhanced surface conjugation of presented proteins, and the particles were also demonstrated to have the capacity for sustained release of a loaded drug. These precisely controllable polymeric particles of micron-size have promise for applications ranging from drug delivery vehicles to devices for cellular immunoengineering. The microfluidic continuous manufacture method of polymeric particle synthesis is a versatile platform for particles composed of different materials and payloads.

Thesis Committee

Jordan J. Green, Ph.D. *(primary advisor, reader)*

Professor, Department of Biomedical Engineering

Johns Hopkins University School of Medicine

Warren L. Grayson, Ph.D. *(reader)*

Professor, Department of Biomedical Engineering

Johns Hopkins University School of Medicine

Joshua C. Doloff, Ph.D. *(reader)*

Assistant Professor, Department of Biomedical Engineering

Johns Hopkins University School of Medicine

Acknowledgements

First of all, I would like to sincerely thank Dr. Jordan J. Green, my mentor and advisor, for introducing me to the world of biomaterials and drug delivery, and for his thoughtful guidance both within and outside the lab. His showing patience, passion and kindness set an example of a great mentor for me, and his profound insights and broad vision in research have been a role model to me and have been a major incentive to me in continuing my future doctoral study. I am grateful to Dr. Green for the overwhelming opportunities he provided and the mentorship he gave that became the solid foundation of my future study and career.

I would also like to thank all of the other professors at the Translational Tissue Engineering Center of Johns Hopkins University – Drs. Jennifer Elisseeff, Kevin Yarema, Hai-Quan Mao, Warren Grayson, Jamie Spangler, Joshua Doloff, Alexander Hillel, Devin O'Brien-Coon and Scott Wilson – for their support. Their excellence in research and teaching broaden my horizons of the fields of biomaterials, tissue engineering and immunoengineering. I especially thank Dr. Grayson and Dr. Doloff for their precious time in reviewing my thesis.

I would not be able to survive the struggles and succeed in my Master's study without the help from everyone in the Green Group – Dr. Stephany Tzeng, Dr. Johan Karlsson, Dr. David Wilson, Yuan Rui, Elana Ben-Akiva, Hannah Vaughan, Kelly Rhodes and Savannah Est. Especially, I'm very grateful to Elana, my direct mentor in research, for her help in teaching me from the very beginning not only in the lab skills but every aspect of conducting research patiently, and for her encouragement and advice in and out of the

lab. Her kindness, and dedication to study and research have profoundly influenced my studies and my life.

When I first came to Baltimore, I had never imagined I would be so privileged to have many supporting friends within the new city and new country. Thank you Zhicheng, Zhiwei, my fellow classmates Haoyang, Luda, Yang, Yunjia, Yuncong, and especially Qingyang, my important one, for your sharing my celebration and consolation at times of both joy and sadness. I'm also grateful to my friends afar, who provided never-ending support in every step along the way, for their everlasting friendship.

Most importantly, I express my heartfelt gratitude to my family. I have been very fortunate to have such loving parents, uncles, aunts and cousins who give me relentless support, blessings, and joy.

Dedication

This thesis is dedicated to my parents, Yingming Yu and Ming Liu, for their eternal love, trust and support.

Table of contents

List of tables

List of figures

Chapter 1

Introduction to the thesis

1.1 Cancer Immunotherapies

Cancer is a leading cause of death and is a major focus for pharmaceutical and biotechnological studies and therapeutic development. Various cancer therapies including surgeries[1], radiotherapies[2], chemotherapies[3], hormone therapies[4] and immunotherapies[5] have been well developed. Among the therapies, immunotherapy is one of the newest and hottest research areas. One of the early demonstrations of utilizing a person's own immune system to fight cancer dates back to the 1980s when William Coley, a young New York surgeon, began intratumoral injection of live or inactivated *Streptococcus pyogenes* and *Serratia marcescens* in an effort to reproduce the spontaneous remissions of sarcomas observed in rare-cancer patients who had developed erysipelas[6]. As part of its normal function, the immune system detects and destroys abnormal cells, including cells that turn into carcinoma. Researchers have found that patients with tumor-infiltrating lymphocytes (TILs), immune cells that are found in and around tumors, often have a better life expectancy[7].

However, cancer cells inherently have the ability to evade monitoring by the immune system through genetic changes that make them less visible, create surface

proteins that turn off immune cells, and/or changing the normal cells around the tumor to create an immunosuppressive microenvironment. The major aim of immunotherapy is to facilitate the endogenous immune system to destroy tumor cells to treat cancers (**Figure 1.1**). Several types of immunotherapies are used to treat cancer, including immune checkpoint blockade[8], T cell transfer therapy[9], monoclonal antibodies[10], and cancer vaccines[11].

Adaptive anti-tumor immune responses must begin with the capture of tumor associated antigens by antigen presenting cells (APCs) such as dendritic cells. To promote the antigen presentation functions of APCs and the production of tumor-specific T cell responses, researchers found that polymeric particle-based synthetic artificial antigen presenting cells (aAPCs) proved to be an effective platform for T cell activation[12, 13]. Further evaluation and characterization of key physical and chemical parameters of aAPCs including size, material composition, shape and surface characteristics could improve aAPC function for T cell activation.

1.2 Polymeric particles based on poly(lactic-co-glycolic acid)

Poly(lactic-co-glycolic acid) (PLGA) is one of the most successfully developed biodegradable polymers. PLGA, whose hydrolysis products are lactic acid and glycolic acid that can be metabolized by the body via the Krebs cycle, has minimal systemic toxicity and has been clinically approved by the US FDA to be used in various drug delivery systems[14] (**Figure 1.2**). By changing the composition of the co-polymer, the degradation time is tunable from several months to several years[15], and PLGA is commercially

available with different molecular weights and co-polymer compositions. The surface of PLGA particles is easy to modify, for example, by PEGylation (coating with a hydrophilic polyethylene glycol (PEG) layer at the surface)[16] or conjugating proteins at the surface[12]. The synthesis method of PLGA particles is easy to set up and modify[12, 17]. The most common technique is the emulsification-solvent evaporation technique (single emulsion). In this technique, PLGA (and hydrophobic payloads) are dissolved in an organic solvent (dichloromethane) and the emulsion, oil (O) in water (W) i.e. O/W, is prepared by adding water and a surfactant (e.g. poly(vinyl alcohol) (PVA)) to the polymer solution. The nano- or micro-sized droplets are induced by sonication or homogenization. The solvent is then evaporated and the particles are collected after washing. A modification of this technique is called double emulsion, which is used to encapsulate hydrophilic drugs (e.g., peptides and proteins) by adding a first W/O emulsion step before the O/W emulsion. The first emulsion step of the combined W/O/W allows hydrophilic payloads dissolved in water to form droplets in PLGA solutions that then subsequently form PLGA-containing droplets in a larger aqueous solution. These characteristics make PLGA particles attractive as versatile platforms for drug delivery, theranostics and vaccines.

The sizes[18], shapes[12], and surfaces[19] of PLGA particles have been engineered and well investigated. However, there is a general lack of precise control over particle size and often large polydispersity in particle size during fabrication following conventional production methods. This creates a challenge to setting standards for particle-based therapies, makes it more difficult for good manufacturing practices, and adds a significant barrier between bench-top research and its translation to the clinic. Renewed efforts to precisely control particle sizes and narrow particle size distributions of PLGA

particles can promote the safe and effective clinical application of more sophisticated biotechnologies and nanomedicine that build upon fundamental particle designs.

1.3 Microfluidic droplet generators

Microfluidics has been described as the science and technology of systems handling small volumes of fluids using micron-sized channels[18]. Microfluidic devices for the generation of microdroplets have led to many applications spanning the food, cosmetic, and pharmaceutical industries, particularly to go beyond the limits of traditionally used emulsification techniques[20-22]. By classifying the internal geometry of channels, microdroplet generators can be categorized into coflowing devices (**Figure 1.3a**), in which the continuous and discontinuous phases (i.e., liquids that will form the emulsion) flow in the same direction at the junction; (ii) flow-focusing devices (**Figure 1.3b**), in which the continuous phase flows from two opposite channels and perpendicularly to the discontinuous phase flow; and (iii) T-junction devices (**Figure 1.3c**), that are similar to the flow-focusing devices except that the continuous phase flows from a single channel. The microfluidic emulsion permits the entrapment of sensitive or poorly water-soluble molecules under soft conditions[23] to generate highly monodisperse droplets (CV lower than 5%) and to reduce the raw materials used[24].

1.4 References

1. Nelson, H., et al., *Guidelines 2000 for colon and rectal cancer surgery.* Journal of the National Cancer Institute, 2001. **93**(8): p. 583-596.
2. Group, E.B.C.T.C., *Effects of radiotherapy and of differences in the extent of surgery for early breast cancer on local recurrence and 15-year survival: an overview of the randomised trials.* The Lancet, 2005. **366**(9503): p. 2087-2106.
3. DeVita, V.T. and E. Chu, *A history of cancer chemotherapy.* Cancer research, 2008. **68**(21): p. 8643-8653.
4. Grodstein, F., P.A. Newcomb, and M.J. Stampfer, *Postmenopausal hormone therapy and the risk of colorectal cancer: a review and meta-analysis.* The American journal of medicine, 1999. **106**(5): p. 574-582.
5. Farkona, S., E.P. Diamandis, and I.M. Blasutig, *Cancer immunotherapy: the beginning of the end of cancer?* BMC medicine, 2016. **14**(1): p. 1-18.
6. McCarthy, E.F., *The toxins of William B. Coley and the treatment of bone and soft-tissue sarcomas.* The Iowa orthopaedic journal, 2006. **26**: p. 154.
7. Clemente, C.G., et al., *Prognostic value of tumor infiltrating lymphocytes in the vertical growth phase of primary cutaneous melanoma.* Cancer: Interdisciplinary International Journal of the American Cancer Society, 1996. **77**(7): p. 1303-1310.
8. Postow, M.A., M.K. Callahan, and J.D. Wolchok, *Immune checkpoint blockade in cancer therapy.* Journal of clinical oncology, 2015. **33**(17): p. 1974.
9. Yee, C., et al., *Adoptive T cell therapy using antigen-specific CD8+ T cell clones for the treatment of patients with metastatic melanoma: in vivo persistence,*

migration, and antitumor effect of transferred T cells. Proceedings of the National Academy of Sciences, 2002. **99**(25): p. 16168-16173.

10. Weiner, L.M., R. Surana, and S. Wang, *Monoclonal antibodies: versatile platforms for cancer immunotherapy.* Nature Reviews Immunology, 2010. **10**(5): p. 317-327.
11. Walter, S., et al., *Multipeptide immune response to cancer vaccine IMA901 after single-dose cyclophosphamide associates with longer patient survival.* Nature medicine, 2012. **18**(8): p. 1254-1261.
12. Meyer, R.A., et al., *Biodegradable nanoellipsoidal artificial antigen presenting cells for antigen specific T-cell activation.* Small, 2015. **11**(13): p. 1519-1525.
13. Sunshine, J.C., et al., *Particle shape dependence of CD8+ T cell activation by artificial antigen presenting cells.* Biomaterials, 2014. **35**(1): p. 269-277.
14. Kumari, A., S.K. Yadav, and S.C. Yadav, *Biodegradable polymeric nanoparticles based drug delivery systems.* Colloids and surfaces B: biointerfaces, 2010. **75**(1): p. 1-18.
15. Vert, M., J. Mauduit, and S. Li, *Biodegradation of PLA/GA polymers: increasing complexity.* Biomaterials, 1994. **15**(15): p. 1209-1213.
16. Owens III, D.E. and N.A. Peppas, *Opsonization, biodistribution, and pharmacokinetics of polymeric nanoparticles.* International journal of pharmaceutics, 2006. **307**(1): p. 93-102.
17. Ben-Akiva, E., et al., *Fabrication of Anisotropic Polymeric Artificial Antigen Presenting Cells for CD8+ T Cell Activation.* JoVE (Journal of Visualized Experiments), 2018(140): p. e58332.

18. Budhian, A., S.J. Siegel, and K.I. Winey, *Haloperidol-loaded PLGA nanoparticles: systematic study of particle size and drug content.* International journal of pharmaceutics, 2007. **336**(2): p. 367-375.

19. Schmid, D., et al., *T cell-targeting nanoparticles focus delivery of immunotherapy to improve antitumor immunity.* Nature communications, 2017. **8**(1): p. 1-12.

20. Babahosseini, H., T. Misteli, and D.L. DeVoe, *Microfluidic on-demand droplet generation, storage, retrieval, and merging for single-cell pairing.* Lab on a chip, 2019. **19**(3): p. 493-502.

21. Lashkaripour, A., et al., *Performance tuning of microfluidic flow-focusing droplet generators.* Lab on a Chip, 2019. **19**(6): p. 1041-1053.

22. Maan, A.A., K. Schroën, and R. Boom, *Monodispersed water-in-oil emulsions prepared with semi-metal microfluidic EDGE systems.* Microfluidics and nanofluidics, 2013. **14**(1-2): p. 187-196.

23. Sanjay, S.T., et al., *Recent advances of controlled drug delivery using microfluidic platforms.* Advanced drug delivery reviews, 2018. **128**: p. 3-28.

24. Duncanson, W.J., et al., *Microfluidic synthesis of advanced microparticles for encapsulation and controlled release.* Lab on a Chip, 2012. **12**(12): p. 2135-2145.

25. Mellman, I., G. Coukos, and G. Dranoff, *Cancer immunotherapy comes of age.* Nature, 2011. **480**(7378): p. 480-489.

26. Doufène, K., et al., *Microfluidic Systems for Droplet Generation in Aqueous Continuous Phases: A Focus Review.* Langmuir, 2019. **35**(39): p. 12597-12612.

1.5 Figures

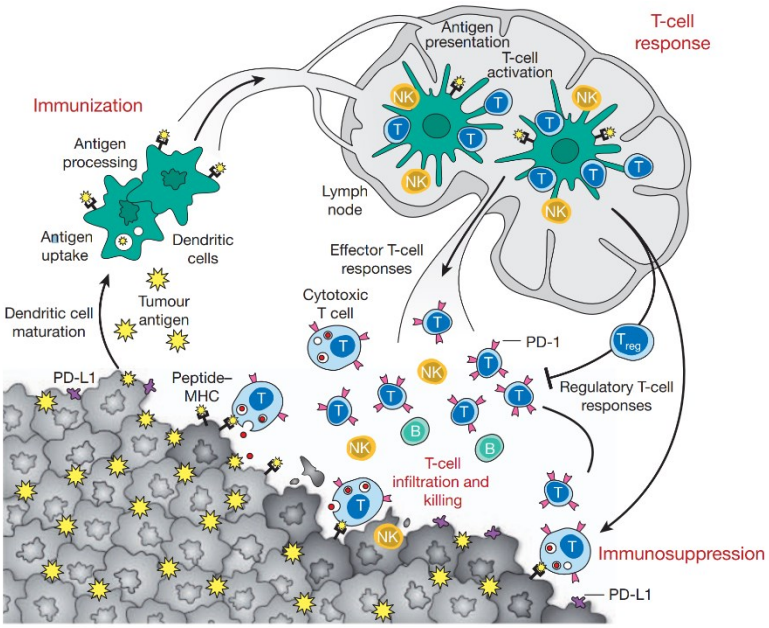

Fig. 1.1. Generation and regulation of antitumor immunity[25]. Understanding the events in generating and regulating antitumor immunity suggests at least three sites for therapeutic intervention: promoting the antigen presentation functions of dendritic cells, promoting the production of protective T-cell responses, and overcoming immunosuppression in the tumor bed.

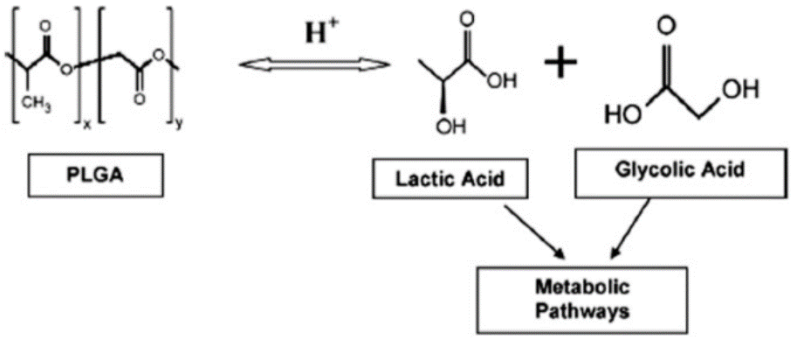

Fig. 1.2. Hydrolysis of PLGA[14]. Hydrolysis products of PLGA are lactic acid and glycolic acid that can be metabolized by the body via Krebs cycle.

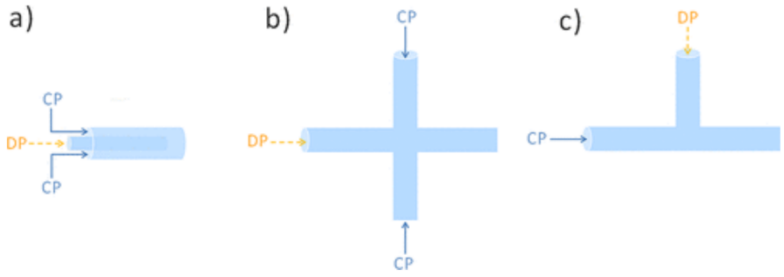

Fig. 1.3. Different designs of microfluidic droplets generators[26]. (a) co-flow device, (b) flow-focusing device, and (c) T-junction device. CP: continuous phase. DP: discontinuous phase.

Chapter 2

Specific Aims

2.1 Overview

This project investigated the effects of different parameters in microfluidic flow focusing devices (MFFDs) to fabricate poly(lactic-co-glycolic acid) (PLGA) microparticles with differentially tuned particle sizes and low polydispersity in particle size for function as therapeutics. The effect of polymer solvent, concentration, flow rates and channel sizes of microfluidic devices on particle sizes was evaluated. Subsequently, biological cell-sized PLGA microparticles were synthesized and functionalized as artificial antigen presenting cells (aAPCs). Broader application of the microfluidic emulsion method to different materials and emulsifications are presented to demonstrate the potential use of MFFDs as a versatile platform for monodisperse particle synthesis.

2.2 Specific Aims

Specific Aim 1. Evaluate the effects of microfluidic device parameters on PLGA microparticle size, polydispersity, and morphology.

Aim 1A. To evaluate the effect of polymer solvent in microfluidic devices on PLGA microparticle morphology.

Aim 1B. To evaluate the effect of polymer concentration in microfluidic devices on particle size of PLGA microparticles.

Aim 1C. To evaluate the effect of microfluidic device channel size on particle size of PLGA microparticles.

Aim 1D. To evaluate the effect of flow rates within microfluidic devices on particle size of PLGA microparticles.

Specific Aim 2. Create monodisperse biodegradable artificial antigen presenting cells (aAPCs).

Aim 2A. Prepare monodisperse PLGA microparticles and evaluate the conjugation of T cell activation proteins to the particle surface to create aAPCs.

Aim 2B. Prepare monodisperse PLGA-based aAPCs with an encapsulated immunoregulatory drug, SD-208, and evaluate encapsulation and sustained release of the loaded aAPCs.

Specific Aim 3. Evaluate broader applications of microfluidic emulsion to different materials and emulsifications.

Aim 3A. Investigate the use of microfluidic emulsion for poly(β-amino ester) (PBAE)-PLGA blend particles.

Aim 3B. Evaluate the potential of microfluidics for W/O/W emulsion.

Chapter 3

Synthesis of monodisperse artificial antigen presenting cells with tunable sizes

3.1 Introduction

Cancer immunotherapy is drawing increased attention for treatment of various cancers such as leukemia[1], melanoma[2], renal cell cancer[3], non-small cell lung cancer[4] and a growing list of other cancers due to impressive and durable response rates. Besides CAR-T therapies and checkpoint blockade therapies, which have shown substantial efficacy in the clinic[5, 6], various preclinical studies demonstrate other promising immunotherapy approaches. Biomimetic artificial antigen presenting cells (aAPCs) can be a promising platform for T cell activation and immune system modulation[7-9]. Artificial antigen presenting cells interact with and activate naïve T cells by displaying T cell activation proteins, usually anti-CD3 or peptide-loaded MHC (signal 1) and co-stimulatory anti-CD28 (signal 2), on the surface of micro- or nanoparticles. The particle-based immune activation strategy provides a platform for complementary approaches, such as using small molecule drugs to modulate intracellular signaling pathways to increase potency and/or increasing the durability of immune-mediated tumor regression from cancer immunotherapies[10-14]. Small molecule transforming growth

factor beta (TGF-beta) inhibitor SD-208 is a great example of a promising small molecule drug for immunotherapy[15]. TGF-beta is a generally immunosuppressive cytokine that is usually overexpressed by tumor cells, inhibiting immune cell proliferation and effective function[16]. Targeted delivery of TGF-beta inhibitors to CD8+ T lymphocytes show efficacy in reversing TGF-beta signaling[15]. As there are known effects of particle size[17], material [18-22] and shape[8, 9] on aAPC efficacy at activating T cells, more progress is needed in controlling the large batch-to-batch variability often observed in aAPC manufacture. Typical existing procedures of micro- and nanoparticles production use bulk emulsion via sonication or mechanical homogenization to generate polymeric particulate materials[8], in which the oil phase containing polymer solution is disturbed in the aqueous phase containing surfactant as a stabilizer. Large polydispersity makes it hard to standardize particle-based therapies, setting a significant barrier for translational application of bench-top research to the clinic. In addition, the upper-end of many particle size distributions can contain large particles that, though relatively few in number, could cause blockage of capillaries following *in vivo* administration. Furthermore, the potential overlap in particle size distributions between differently designed batches obscures precise study of the effects of particles size on the efficacy of particle-based therapies.

Microfluidic droplet generators, used in quick diagnosis[23, 24], single cell analysis[25], and cell encapsulation[26], can inherently generate monodispersed droplets. Studies show that microfluidic devices can produce monodisperse polymeric particles of micron-scale sizes[27-29], providing a low-cost and easy-to-use platform for emulsification. The commonly used droplet generating microfluidic devices include co-flow devices, T-junction devices[30] and flow focusing devices[26]. Flow focusing devices

have been used to synthesize photocurable polymeric particles[29, 31], ion-crosslinkable thermosensitive gels[32], polymer-encapsulated cells[33], and other particles[27]. In previous studies, the drug release kinetics from the particles generated by microfluidic devices was well studied[31]. However, the application of monodisperse microparticles to immune engineering and the comparison between the efficacy of aAPCs based on monodisperse particles rather than polydisperse particles has not been well-studied. To enhance efficacy, safety, reproducibility, and scale-up, it would be interesting to evaluate aAPCs fabricated via classic bulk emulsion compared to aAPCs fabricated via microfluidic devices.

In this chapter, we describe the fabrication of monodisperse, biodegradable, SD-208-loaded microparticles and functionalization of these particles into aAPCs. Our objective in this research was to demonstrate the manufacture of monodisperse and scalable aAPCs and to compare them to bulk-emulsion aAPCs. We hypothesize that monodisperse microparticles made by microfluidic flow focusing devices may have improved efficacy and utility as aAPCs.

3.2 Materials and Methods

Fabrication of microfluidic devices: We fabricated the microfluidic channels using soft lithography[37]. The height of each device was 100 mm. We sealed the plasma-oxidized PDMS mold against an oxidized glass slide (Corning); it was necessary to plasma oxidize the surfaces of both the PDMS and the glass before bringing them into contact to make covalent bonds[33]. In order to avoid the wetting of the dispersed phase to the inner surface

of the device and to induce stable hydrophilicity of the channel walls[34], a pretreatment of the channels was performed by prefilling the channels with 1% PVA (25kDa) (Sigma Aldrich; St. Louis, MO) solution for 30 minutes and washing out the PVA via air blowing and heat drying immediately after sealing the PDMS mold to the glass slide.

Fabrication of PLGA monodisperse microparticles using microfluidic devices: We followed reported procedures to synthesize PLGA microparticles using microfluidic flow focusing devices (MFFDs)[28]. Briefly, poly (lactic-co-glycolic acid) acid terminated (38-54 kDa, 50:50 L:G ratio) (PLGA, Sigma Aldrich; St. Louis, MO) was used as the core material for particle synthesis. The PLGA was dissolved at desired concentrations in dichloromethane (DCM) or ethyl-acetate to form the dispersed phase solution in the MFFDs. For SD-208 drug release studies, particles were loaded with SD-208 (Cayman Chemical; Ann Arbor, MI) at a 10% mass ratio (wt/wt) of the drug to the polymer. Teflon tubing (Cole Parmer; Vernon Hills, IL) was used to connect the syringe and inlets on the device. Automatic syringe pumps (Cole Parmer, Vernon Hills, IL) were used to provide steady flow rates for both the dispersed phase and continuous phase. For the studies on the effects of dispersed phase solvent, PLGA was dissolved in DCM or ethyl acetate at 20 mg/mL. MFFDs with 50 μm channel size were used and the flow rates of dispersed phase and continuous phase was set at 1 mL/hr and 10 mL/hr, respectively. For the studies on the effects of polymer concentration on particle sizes, PLGA was dissolved at 2 mg/mL, 10 mg/mL and 20 mg/mL, respectively, in DCM. MFFDs with 100 μm channel size were used and the flow rates of dispersed phase and continuous phase was set at 1 mL/hr and 10 mL/hr, respectively. For the study on the effects of channel sizes on particle sizes, MFFDs

with 100 μm and 50 μm channel sizes were used. For these studies, two different sets of parameters were used: PLGA was dissolved at 20 mg/mL in DCM and the flow rates of dispersed phase and continuous phase was set to 1 mL/hr and 10 mL/hr, respectively; PLGA was dissolved at 2 mg/mL in DCM and the flow rates of dispersed phase and continuous phase was set to 0.5 mL/hr and 15 mL/hr, respectively. For the study of effects of flow rate ratio on particle sizes, PLGA was dissolved at 2 mg/mL in DCM. MFFDs with 100 μm channel size were used and the flow rate of dispersed phase was set to 0.5 mL/hr as a constant. For these experiments, the flow rate of the continuous phase was varied to be either 5 mL/hr, 10 mL/hr, or 15 mL/hr, respectively. Droplets were collected in a 250 mL beaker prefilled with 50 mL of continuous phase solution on a stir plate. The buffer in the collecting beaker was stirred while collecting particle droplets to minimize potential aggregation. The generated droplets were incubated in the beaker overnight to allow the dispersed phase solvent to evaporate and the particles to harden. The particles were then washed three times with deionized water at 3,200 g for 5 minutes, frozen and lyophilized.

Bulk PLGA microparticle synthesis: Polymeric nanoparticles were synthesized using single emulsion techniques as previously described[8, 38]. PLGA was dissolved at 20 mg/mL in DCM and 5 mL of the polymer solution was then emulsified in 50 mL of 1% polyvinyl alcohol (PVA) solution using a homogenizer (IKA-3725001; Wilmington, NC) set to 3.2k rpm for 1 minute. The resulting emulsification was poured into 100 mL of a 0.5% PVA solution on a magnetic stir plate at 500 rpm and the particles were allowed to harden for at least 4 hours. The particles were centrifuged at 3200 g for 5 minutes to pellet out

microparticles. The supernatant was collected and washed three times with deionized water at 40,000 g for 15 minutes, frozen and lyophilized.

Protein conjugation: EDC-NHS chemistry was used to conjugate T cell-binding and activation proteins anti-CD3 and anti-CD28 onto the surface of monodisperse PLGA microparticles made by MFFDs. The conjugation procedures were modified based on established methods[8]. The particles were briefly incubated in 1 M NaOH solution (pH ~14) to degrade the surface and expose additional carboxylic acid groups on the surface. 1 N HCl solution (pH~0.1) was added to quench the pre-degradation. The particles were incubated in 4-morpholinoethanesulfonic acid (MES) buffer containing 1-ethyl-3-(3-dimethylaminopropyl)carbodiimide hydrochloride (EDC) and N-hydroxysulfosuccinimide (sulfo-NHS) for 30 minutes. Then, Syrian hamster anti-mouse-CD28 (Clone 37.51, BioLegend; San Diego, CA) in 100 μL 1X PBS was added at a dose of 10 μg per mg particles. After a 3-hour reaction with anti-CD28, rat anti-mouse-CD3 (Clone 17A2, BioLegend; San Diego, CA) was added at a dose of 8 μg per mg particles. After an overnight reaction between the antibodies and microparticles, the microparticles were washed three times to remove the residual free antibodies that did not attach to the microparticles. In order to quantify the amount of anti-CD3 and anti-CD28 antibodies on the surface of the particles, Alexa Fluor™ 488 labeled anti-rat antibody and Alexa Fluor™ 647 labeled anti-hamster antibody were used (BioLegend; San Diego, CA). Particles were incubated with a cocktail of two antibodies for 30 minutes at room temperature in 1X PBS at 2 mg/mL of each antibody. Following incubation, the particles were washed three times

in 1X PBS at 3,200 g for 5 minutes and read on a BioTek Synergy 2 plate reader (BioTek; Winooski, VT).

SD-208 release studies: Two mg of the particles loaded with SD-208 were dissolved in 1 mL Dimethyl sulfoxide (DMSO) to quantify the encapsulation efficiency. The absorbance at 570 nm was measured on a BioTek Synergy 2 plate reader (BioTek; Winooski, VT). In order to characterize drug release profile, SD-208 loaded particles were incubated in 1X PBS at 2 mg/mL. On days 1, 2, 3, 4, 8 and 12, the particles were centrifuged at 3,200 g for 5 minutes to pellet out microparticles. The supernatant was collected and the absorbance measured on a BioTek Synergy 2 plate reader (BioTek; Winooski, VT).

Characterization of PLGA microparticles: Microparticles made by bulk emulsion and MFFDs were imaged under scanning electron microscopy (SEM) using a LEO/Zeiss Field-emission SEM. The sizes of microparticles were measured manually using ImageJ[39].

Statistics: All experiments were performed with n = 3 replicates unless otherwise stated. Bar graphs indicate mean ± standard error of the mean. n.s. (not significant) indicates $p > 0.05$, * indicates $p \leqslant 0.05$, ** indicates $p \leqslant 0.01$, *** indicates $p \leqslant 0.001$, and **** indicates $p \leqslant 0.0001$. All statistics were completed using statistical analysis software modules in GraphPad Prism 8 (GraphPad Software, Inc.; La Jolla, CA). For particle size measurements, a Student's t-test was used to assess the difference between particles made by MFFDs of different channel sizes. Student's t-test was also used in the comparison between PLGA microparticles made by bulk emulsion and monodisperse microparticles

made by MFFDs. In all cases, differences were considered significant if the p-value of the test was less than 0.05.

3.3 Results

3.3.1 The effect of polymer solvent on microparticle morphology

We used flow focusing droplet generator to produce monodisperse microparticles. In a flow focusing design, the dispersed phase is introduced directly into the main channel while the continuous phase is injected and divided into two branches placed perpendicularly[28]. The dispersed phase, which is polymer in its solvent, is then pinched on both sides by the continuous phase, which is water with surfactant to prevent particle aggregation, and a droplet is formed due to the competition between the viscous forces and the surface tension at the interface between the two phases. The successful operation of flow focusing devices relies on hydrophilicity of the channel walls[31]. However, polydimethylsiloxane (PDMS), which allows easy manufacture of microfluidic devices, is inherently hydrophobic. Thus, a dispersed phase containing PLGA would eventually wet the sidewall of PDMS devices, preventing the formation of discrete droplets and thus particles and limiting the durability of such a device. Therefore, to induce stable hydrophilicity of the channel walls[34], a pretreating methods was used by prefilling the channels with a 1% PVA solution and washing out the PVA via air blowing and heat drying.

In order to operate our microfluidic devices to produce monodisperse microparticles, we followed previously reported methods[28]. Briefly, polytetrafluoroethylene (PTFE) tubing connected the syringe and inlets on the device. Automatic syringe pumps were used to provide steady flow rate for both the dispersed

phase and the continuous phase. Droplets were collected in a beaker prefilled with continuous phase solution on a stir plate (**Figure 3.1**). The buffer in the collecting beaker was stirred while collecting the particles to minimize potential aggregation. The generated droplets were incubated in the beaker overnight to allow the dispersed phase solvent to evaporate. The particles were then centrifuged, washed three times with water, and lyophilized to generate dried microspheres.

We used two different polymer solvents to dissolve PLGA and compared the morphologic characteristics of particles prepared from each method. Dichloromethane (DCM) was used as a traditional solvent for PLGA nano- and micro- particle production. PLGA was dissolved in DCM in 20 mg/mL as the dispersed phase for use in our microfluidic devices. 1% PVA water solution was used as continuous phase. The flow rates of dispersed phase and continuous phase was kept constant. The obtained PLGA microparticles were imaged under the scanning electron microscopy (SEM) to characterize the size and monodispersity of the particles.

Although DCM is generally viewed as a good polymer solvent that is widely used in polymeric particle synthesis, the inherent hydrophobicity was found to wet the channel walls of the microfluidic device, preventing consistent production of monodisperse microparticles and decreasing the durability of the devices. It has been reported that some partially water-miscible solvents such as ethyl-acetate can be used for polymeric nano- and micro- particle synthesis as well[35]. The partial water miscibility of ethyl acetate decreases the occurrence of hydrophobic wetting of the dispersed phase solution when used as PLGA solvent in microfluidic flow focusing devices.

We used the same parameters (PLGA concentration, flow rate, and channel size) as to compare the shapes of microparticles produced from ethyl acetate as the dispersed phase compared to DCM. SEM images showed that the PLGA microparticles produced with DCM as the dispersed phase were spherical (**Figure 3.2**), like the microparticles made by traditional bulk emulsion (**Figure 3.3**). The PLGA microparticles produced by ethyl acetate as the dispersed phase, however, had a dimple shape with a indentation in the center of each disk instead (**Figure 3.4**).

A possible reason for the anisotropic shape is that ethyl acetate has a lower volatility than dichloromethane, and ethyl-acetate will evaporate more slowly during the formation of microparticles. The formation of microparticles requires the polymer solvent that composes the emulsion droplets to diffuse to the water-droplet interface and evaporate[36]. Subsequently, the increased concentration of polymer within a smaller droplet will cause the separation of solvent and polymer and the hardening of the polymeric particles. The smaller evaporation speed of ethyl acetate makes the hardening of PLGA particles occur more slowly. With the slower diffusion and evaporation of ethyl acetate, PLGA accumulates at the solvent-water interface and solidifies. As phase separation occurs, a PLGA shell forms. However, the solvent (ethyl acetate) that remains in the droplets has to be released. Under the effects of gravity, the upper part of the newly formed PLGA shell is the most fragile section of the polymer shell. The remaining solvent can break this upper part of the shell to release from the droplet, and thus the dimple forms.

Although ethyl acetate as a PLGA solvent can prolong the durability of microfluidic flow focusing devices, it inevitably makes the microparticles form an anisotropic dimple

shape. Due the forces driving the dimple formation, the larger the gravitational influence and the larger the microparticle size, the more pronounced the dimple shape they will be.

3.3.2 The effects of polymer concentration on microparticle size and monodispersity

As the ethyl acetate solvent will cause microparticles to be dimple-shaped, we used dichloromethane as the solvent so that the spherical microparticles can have a controlled, isotropic shape. Microparticles were produced following the same procedures using microfluidic flow focusing devices as described above. We used PLGA in DCM at different concentrations as the dispersed phase and 1% PVA in water as the continuous phase. The other parameters, including flow rates and the design of the MFFDs, was maintained constant. SEM imaging was used to image the produced microparticles to measure the effects of polymer concentration on the size and polydispersity of the particles.

Here we induce a parameter, coefficient of variation (CV), to quantify the polydispersity of microparticles, which is defined as the ratio between the standard deviation and the mean of the particle diameter multiplied by 100. The particle diameters of the microparticles were quantified manually after imaging via SEM. The monodisperse PLGA microparticles were found to have a small CV of approximately 5%. As comparison, we also made PLGA microparticles via typical bulk emulsion and imaged the particles via SEM. The microparticles fabricated by bulk emulsion had a CV up to 30%. Different PLGA concentrations used in the preparation of the PLGA microparticles did not change

the monodispersity of produced microparticles significantly, and the CV remained approximately 5% (**Table 3.1**).

However, by using MFFDs of the same design and channel size, as the PLGA concentration increases, the particle sizes of the microparticles increases (**Table 3.1 and Figure 3.5**). The increase in microparticle sizes can be interpreted as the result of increased polymer concentration in the formed droplet. The increased amount of PLGA contained in each droplet causes the hardened microparticle formed by each droplet to be larger. Good reproducibility was found using the microfluidic flow focusing devices to produce droplets and particles of the desired size, with PLGA concentration being an important parameter to tune particle size while maintaining monodispersity.

3.3.3 The effect of channel size on microparticle size and monodispersity

Similarly to the study of the effects of polymer concentration on microparticle sizes and monodispersity, we used PLGA in DCM as the dispersed phase and a 1% PVA solution as continuous phase to investigate the role of channel size. Here we chose the parameters that previously generated relatively large particles and used microfluidic flow focusing devices of two different channel sizes to explore the role of channel size, focusing on the size of the channel at the intersection of the continuous phase and the dispersed phase.

After SEM imaging and quantifying the sizes and polydispersity of the images, the generated microparticles were found to maintain good monodispersity in both of the groups studied. We observed similar monodispersity between the two channel sizes for microparticle production and the CV of the microparticles produced was approximately 5%

(**Table 3.2**), consistent with the study above. Using the same polymer concentration and flow rate, the microparticles made by the MFFD with the larger channel produced larger particle sizes compared with the particles that the smaller sized channel produced (**Table 3.2 and Figure 3.6**).

However, when we subsequently used another set of parameters (higher continuous phase flow rate and lower dispersed phase flow rate to make smaller particles) to repeat the experiment, we found that channel size has a limited ability to tune particle size smaller beyond a critical size threshold. The new device parameters were set to produce smaller microparticles and the MFFDs of the same design with two different channel sizes were used. The results showed that the monodispersity of the microparticles was consistent with CVs of 5% (**Table 3.3**). However, with these new device settings there was not a significant difference between the particle sizes of the microparticles produced using MFFDs of the two different channel sizes (**Table 3.3, Figure 3.7 and Figure 3.8**).

The observed phenomena is likely due to relative length scales between the droplet size and the channel size. Generally, for larger microparticles, a smaller channel size decreases the sizes of the droplets (and subsequent microparticles) that the device makes. However, due to flow conditions the generated droplets are significantly smaller than both sizes of the channels, as in the second experiment, the channel sizes have limited influence on particle size.

3.3.4 The effects of flow rate ratio on microparticle size and monodispersity

The effects of polymer concentration and channel size of microfluidic flow focusing devices on microparticle size and monodispersity were studied above. To make the devices more versatile to produce particles of different size, the parameter that is the easiest for a user to tune is the flow rate. The flow rate can be manipulated by changing the setting of the syringe pumps rather than by fabricating different devices or preparing PLGA-DCM solutions of different concentrations. To study the effects of flow rate (especially the flow rate ratio of the dispersed phase to the continuous phase), we kept parameters other than flow rates constant. First, the flow rate of the dispersed phase was set constant and the flow rate of the continuous phase was manipulated.

The results of SEM imaging and image quantification revealed that when the flow rate of the dispersed phase remained unchanged, by changing the flow rate of the continuous phase the generated monodisperse microparticle had different size, with higher flow rates leading to smaller particle size (**Figure 3.9**). As before, the monodispersity remained low with a CV of approximately 5% (**Table 3.4**).

In summary, by tuning certain key parameters during particle production, including the channel size of MFFDs, the flow rate ratio of the dispersed phase to the continuous phase, and concentration of PLGA in the dispersed phase, we obtained microparticles of different tunable sizes (from ~7 μm to ~50 μm), and the polydispersity remained low regardless of microparticle size (CV ~5%) (**Table 3.5**). While large microparticles are typically desired for drug delivery depots due to their large drug loading capacity, we desired to engineer small, monodisperse microparticles that were approximately the same

size as biologic cells and capable of multiple routes of *in vivo* administration[1]. By engineering MFFDs and tuning multiple fabrication parameters, consistent monodisperse isotropic microparticles of biomimetic size were successfully generated.

3.3.5 *In vitro* drug release and protein conjugation

Among the library of monodisperse microparticles of different sizes, we selected cell-sized, small microparticles (monodisperse microparticles of 7 μm) to be further investigated, as these sized particles match the classical design of aAPCs and allow for multiple modes of administration *in vivo*. It has been reported that the smallest capillaries in adults are approximately 7 μm [40]. A larger spherical particle means a larger surface area to present proteins to interact with T cells as well as a larger volume to encapsulate and release immunomodulatory molecules, both properties capable of boosting the efficacy of aAPCs. Thus, an ideal particle size range for aAPC design is at or just under this smallest capillary limit.

In order to functionalize the monodisperse microparticles, T cell-binding and activation proteins, anti-CD3 as signal 1 and anti-CD28 as signal 2, were conjugated on the surface of particles via EDC-NHS[8]. Briefly, the particles were incubated in 4-morpholinoethanesulfonic acid (MES) buffer containing 1-ethyl-3-(3-dimethylaminopropyl)carbodiimide hydrochloride (EDC) and N-hydroxysulfosuccinimide (sulfo-NHS). Then a cocktail of mouse anti-CD3 and anti-CD28 was added and the antibodies and microparticles reacted overnight before washing out the residual free antibodies that did not become conjugated to the microparticles. Fluorescent secondary

antibodies were used to quantify the protein amount of each protein on the surface. The fluorescence was measured via a fluorescence plate reader.

Low protein conjugation was observed on the surface of the microparticles following the conventional EDC-NHS conjugation procedure (**Figure 3.10**). The low conjugation efficiency was likely a result of residual PVA surfactant coating on the surface of the microparticles following microfluidic fabrication. Such a coating could cover the reactive carboxylic acid surface groups and hinder the formation of linkages between carboxyls on the particle surface and amines on the proteins. In addition, we also observed more anti-CD3 protein on the surface after conjugation than anti-CD28 protein. Therefore, we next modified the coupling procedure such that we first incubated the microparticles in a NaOH solution to degrade the particle surface and expose more carboxylic acid groups. For coupling, anti-CD28 protein in PBS buffer was firstly added to the particles and given a 3-hour incubation time alone before anti-CD3 protein was subsequently added to the reaction. As before, protein coupling was quantified by secondary fluorescent antibodies and a fluorescence plate reader.

Compared with the original conjugation procedure, the modified conjugation procedure improved conjugation efficiency, increased amount of both proteins on the surface, and improved the ratio of the two proteins to be closer to unity (**Figure 3.11**). Further, the monodisperse microfluidically-prepared microparticles also had a higher amount of both proteins conjugated to their surface compared with microparticles of similar size fabricated by conventional bulk emulsion (**Figure 3.12**). The molar ratio of anti-CD3 (signal 1) to anti-CD28 (signal 2) was approximately 1, as desired, indicating a relatively equal amount of two signals necessary for T cell activation.

To boost potential T cell activation function further and to break a potentially immunosuppressive microenvironment, we also incorporated SD-208[15], which is a hydrophobic small molecule TGF-beta inhibitor, into the microparticles. To quantify drug encapsulation, we dissolved the drug loaded particles and measured the absorbance of SD-208. The results show approximately 80% efficiency of the added drug being successfully loaded into the particles (**Figure 3.13**). In general, the drug was released from the PLGA microparticles in a sustained manner (**Figure 3.14**), in accordance with literature describing similar release of small hydrophobic drug molecules from PLGA particles[28].

3.4 Conclusion and Discussion

In this work, polymeric microparticles of tunable size with excellent monodispersity, reproducibility, and scalability have been developed through microfluidic flow focusing devices. Further, we have successfully demonstrated that monodisperse biodegradable polymeric microparticles of cell-like biomimetic size can be successfully functionalized as artificial antigen presenting cells (aAPCs) by the conjugation of a signal 1 and signal 2 to the surface and can also encapsulate and release immunomodulatory molecules. Through modification of microfluidic flow focusing device parameters such as polymer concentration, flow rate ratio of the dispersed to continuous phases, and channel sizes of the devices, we have demonstrated the ability to tune particle size by approximately an order of magnitude while maintaining excellent monodispersity. To demonstrate proof-of-concept, we functionalized monodisperse microparticles made by the devices into biomimetic aAPCs by conjugating T cell activation proteins anti-CD3 and anti-CD28 on

the surface and incorporating the small molecule immunomodulatory drug SD-208 into the particles. In addition to narrow size distribution and scalability, our monodisperse microparticles exhibit increased protein conjugation efficiency compared with microparticles prepared by bulk emulsion. The low variability between batches in synthesis makes it possible to standardize the particle-based therapies as drug delivery vehicles and as aAPCs. The continuous manufacturing methods are easily scalable by simply running the devices for a longer time, unlike with batch manufacturing methods. Future directions to enhance biomimicry would likely further improve aAPC function including double emulsion methods using microfluidic devices for encapsulation of hydrophilic proteins, continued investigation into particle shape, and exploration of broader materials for aAPC construction. Overall, these methods demonstrate a versatile and translatable approach towards the manufacture of precise monodisperse microparticles for immunoengineering, cancer therapy, and other applications.

3.5 References

1. Davila, M.L. and R.J. Brentjens, *CD19-Targeted CAR T cells as novel cancer immunotherapy for relapsed or refractory B-cell acute lymphoblastic leukemia.* Clinical advances in hematology & oncology: H&O, 2016. **14**(10): p. 802.
2. Tran, E., et al., *Cancer immunotherapy based on mutation-specific CD4+ T cells in a patient with epithelial cancer.* Science, 2014. **344**(6184): p. 641-645.
3. Coppin, C., et al., *Immunotherapy for advanced renal cell cancer.* Cochrane database of systematic reviews, 2004(3).
4. Hariu, H., et al., *Aberrant expression and potency as a cancer immunotherapy target of inhibitor of apoptosis protein family, Livin/ML-IAP in lung cancer.* Clinical cancer research, 2005. **11**(3): p. 1000-1009.
5. Ott, P.A., F.S. Hodi, and C. Robert, *CTLA-4 and PD-1/PD-L1 blockade: new immunotherapeutic modalities with durable clinical benefit in melanoma patients*. 2013, AACR.
6. Park, J.H., M.B. Geyer, and R.J. Brentjens, *CD19-targeted CAR T-cell therapeutics for hematologic malignancies: interpreting clinical outcomes to date.* Blood, The Journal of the American Society of Hematology, 2016. **127**(26): p. 3312-3320.
7. Maus, M.V., et al., *Ex vivo expansion of polyclonal and antigen-specific cytotoxic T lymphocytes by artificial APCs expressing ligands for the T-cell receptor, CD28 and 4-1BB.* Nature biotechnology, 2002. **20**(2): p. 143-148.
8. Meyer, R.A., et al., *Biodegradable nanoellipsoidal artificial antigen presenting cells for antigen specific T-cell activation.* Small, 2015. **11**(13): p. 1519-1525.

9. Sunshine, J.C., et al., *Particle shape dependence of CD8+ T cell activation by artificial antigen presenting cells.* Biomaterials, 2014. **35**(1): p. 269-277.

10. Bhavna, et al., *Preparation, characterization, in vivo biodistribution and pharmacokinetic studies of donepezil-loaded PLGA nanoparticles for brain targeting.* Drug development and industrial pharmacy, 2014. **40**(2): p. 278-287.

11. Choi, H.S., et al., *Design considerations for tumour-targeted nanoparticles.* Nature nanotechnology, 2010. **5**(1): p. 42.

12. Gao, X., et al., *In vivo cancer targeting and imaging with semiconductor quantum dots.* Nature biotechnology, 2004. **22**(8): p. 969-976.

13. Tao, Z., et al., *Biological imaging using nanoparticles of small organic molecules with fluorescence emission at wavelengths longer than 1000 nm.* Angewandte Chemie International Edition, 2013. **52**(49): p. 13002-13006.

14. Ye, F., et al., *Biodegradable polymeric vesicles containing magnetic nanoparticles, quantum dots and anticancer drugs for drug delivery and imaging.* Biomaterials, 2014. **35**(12): p. 3885-3894.

15. Schmid, D., et al., *T cell-targeting nanoparticles focus delivery of immunotherapy to improve antitumor immunity.* Nature communications, 2017. **8**(1): p. 1-12.

16. Park, K., et al., *Genetic changes in the transforming growth factor beta (TGF-beta) type II receptor gene in human gastric cancer cells: correlation with sensitivity to growth inhibition by TGF-beta.* Proceedings of the National Academy of Sciences, 1994. **91**(19): p. 8772-8776.

17. Mescher, M.F., *Surface contact requirements for activation of cytotoxic T lymphocytes.* The Journal of Immunology, 1992. **149**(7): p. 2402-2405.

18. Engelhard, V.H., et al., *Induction of secondary cytotoxic T lymphocytes by purified HLA-A and HLA-B antigens reconstituted into phospholipid vesicles.* Proceedings of the National Academy of Sciences, 1978. **75**(11): p. 5688-5691.

19. Giannoni, F., et al., *Clustering of T cell ligands on artificial APC membranes influences T cell activation and protein kinase C θ translocation to the T cell plasma membrane.* The Journal of Immunology, 2005. **174**(6): p. 3204-3211.

20. Oelke, M., et al., *Ex vivo induction and expansion of antigen-specific cytotoxic T cells by HLA-Ig–coated artificial antigen-presenting cells.* Nature medicine, 2003. **9**(5): p. 619-625.

21. Perica, K., et al., *Nanoscale artificial antigen presenting cells for T cell immunotherapy.* Nanomedicine: Nanotechnology, Biology and Medicine, 2014. **10**(1): p. 119-129.

22. Ugel, S., et al., *In vivo administration of artificial antigen-presenting cells activates low-avidity T cells for treatment of cancer.* Cancer research, 2009. **69**(24): p. 9376-9384.

23. Hatakeyama, T., D.L. Chen, and R.F. Ismagilov, *Microgram-scale testing of reaction conditions in solution using nanoliter plugs in microfluidics with detection by MALDI-MS.* Journal of the American Chemical Society, 2006. **128**(8): p. 2518-2519.

24. Zheng, B., L.S. Roach, and R.F. Ismagilov, *Screening of protein crystallization conditions on a microfluidic chip using nanoliter-size droplets.* Journal of the American chemical society, 2003. **125**(37): p. 11170-11171.

25. Joensson, H.N. and H. Andersson Svahn, *Droplet microfluidics—A tool for single-cell analysis.* Angewandte Chemie International Edition, 2012. **51**(49): p. 12176-12192.

26. Collins, D.J., et al., *The Poisson distribution and beyond: methods for microfluidic droplet production and single cell encapsulation.* Lab on a Chip, 2015. **15**(17): p. 3439-3459.

27. Karnik, R., et al., *Microfluidic platform for controlled synthesis of polymeric nanoparticles.* Nano letters, 2008. **8**(9): p. 2906-2912.

28. Xu, Q., et al., *Preparation of monodisperse biodegradable polymer microparticles using a microfluidic flow-focusing device for controlled drug delivery.* Small, 2009. **5**(13): p. 1575-1581.

29. Zhang, H., et al., *Microfluidic production of biopolymer microcapsules with controlled morphology.* Journal of the american chemical society, 2006. **128**(37): p. 12205-12210.

30. Thorsen, T., et al., *Dynamic pattern formation in a vesicle-generating microfluidic device.* Physical review letters, 2001. **86**(18): p. 4163.

31. Xu, S., et al., *Generation of monodisperse particles by using microfluidics: control over size, shape, and composition.* Angewandte Chemie International Edition, 2005. **44**(5): p. 724-728.

32. Kim, J.W., et al., *Fabrication of monodisperse gel shells and functional microgels in microfluidic devices.* Angewandte chemie international edition, 2007. **46**(11): p. 1819-1822.

33. Tan, W.H. and S. Takeuchi, *Monodisperse alginate hydrogel microbeads for cell encapsulation.* Advanced materials, 2007. **19**(18): p. 2696-2701.

34. Trantidou, T., et al., *Hydrophilic surface modification of PDMS for droplet microfluidics using a simple, quick, and robust method via PVA deposition.* Microsystems & nanoengineering, 2017. **3**(1): p. 1-9.

35. Yang, E., et al., *Microfluidic Preparation of Liposomes Using Ethyl Acetate/n-Hexane Solvents as an Alternative to Chloroform.* Journal of Chemistry, 2018. **2018**.

36. Im, S.H., U. Jeong, and Y. Xia, *Polymer hollow particles with controllable holes in their surfaces.* Nature materials, 2005. **4**(9): p. 671-675.

37. Love, J.C., J.R. Anderson, and G.M. Whitesides, *Fabrication of three-dimensional microfluidic systems by soft lithography.* Mrs Bulletin, 2001. **26**(7): p. 523-528.

38. Ben-Akiva, E., et al., *Fabrication of Anisotropic Polymeric Artificial Antigen Presenting Cells for CD8+ T Cell Activation.* JoVE (Journal of Visualized Experiments), 2018(140): p. e58332.

39. Schneider, C.A., W.S. Rasband, and K.W. Eliceiri, *NIH Image to ImageJ: 25 years of image analysis.* Nature methods, 2012. **9**(7): p. 671-675.

40. Romanowsky, M.B., et al., High throughput production of single core double emulsions in a parallelized microfluidic device. Lab on a Chip, 2012. 12(4): p. 802-807.

3.6 Tables

	[PLGA] = 20 mg/mL	[PLGA] = 10 mg/mL	[PLGA] = 2 mg/mL	[PLGA] = 20 mg /mL bulk emulsion
Size (Mean ± SD)	51 ± 3 µm	32 ± 2 µm	22 ± 1 µm	8 ± 3 µm
Coefficient of Variation	5.87%	5.87%	4.82%	34.2%

Table 3.1. PLGA microparticle size and polydispersity as a function of polymer concentration and manufacturing procedure. By using MFFDs of the same design and channel size, as the PLGA concentration increases from 2 mg/mL to 20 mg/mL, the size of microparticles increases from 20 µm to 50 µm, with particles demonstrating excellent monodispersity with a CV of approximately 5%.

Channel size	50 µm	100 µm	[PLGA] = 20 mg /mL bulk emulsion
Size (Mean ± SD)	30 ± 2 µm	51 ± 3 µm	8 ± 3 µm
Coefficient of Variation	5.01%	5.87%	34.2%

Table 3.2. PLGA microparticle size and polydispersity as a function of channel size in microfluidic devices for large particles. By using MFFDs of the same design, polymer concentration and flow rate, the smaller sized channel (50 µm) generated smaller microparticles with an average size of 30 µm compared to a larger size 100 µm channel that generated 51 µm-sized particles. All of the particles had excellent monodispersity with a CV of approximately 5%.

Channel size	50 µm	100 µm	[PLGA] = 20 mg /mL bulk emulsion
Size (Mean ± SD)	7.5 ± 0.4 µm	7.7 ± 0.6 µm	8 ± 3 µm
Coefficient of Variation	5.72%	7.20%	34.2%

Table 3.3. PLGA microparticle size and polydispersity as a function of channel size in microfluidic devices for small particles. By using MFFDs of the same design, polymer concentration and flow rate, to create smaller sized particles an order of magnitude reduced in comparison to channel size, channel size by itself was found to not significantly influence particle size. With the smaller channel 50 µm size, particle size and CV was only very slightly smaller than with the larger 100 µm channel size.

Continuous phase flow rate	5 mL/hr	10 mL/hr	15 mL/hr	[PLGA] = 20 mg/mL bulk emulsion
Size (Mean ± SD)	22 ± 1 µm	12.8 ± 0.6 µm	7.5 ± 0.4 µm	8 ± 3 µm
Coefficient of Variation	5.87%	4.78%	5.72%	34.2%

Table 3.4. PLGA microparticle size and polydispersity as a function of flow rate ratio. The results of SEM imaging and quantitative image analysis showed that when the flow rate of the dispersed phase remained at 0.5 mL/hr, by tuning the flow rate of the continuous phase between 5 mL/hr, 10 mL/hr and 15 mL/hr, the generated monodisperse microparticle had average sizes of 22 µm, 13 µm and 7.5 µm. The polydispersity remained low with a CV of approximately 5%.

Device	Flow rate C:D (mL/hr)	[PLGA] = 20 mg/mL	[PLGA] = 10 mg/mL	[PLGA] = 2 mg/mL
100 µm channel	5:0.5	51 ± 3 µm	32 ± 2 µm	22 ± 1 µm
	10:0.5	/	/	12.2 ± 0.6 µm
	15:0.5	/	/	7.7 ± 0.6 µm
50 µm channel	5:0.5	31 ± 2 µm	/	/
	10:0.5	/	/	12.8 ± 0.7 µm
	15:0.5	/	/	7.5 ± 0.4 µm
Control	3.2k rpm	8 ± 3 µm (20 mg/mL)		

Table 3.5. Summary of PLGA microparticle size and polydispersity from different manufacturing methods. The size and polydispersity of microparticles can be tuned by key parameters of MFFDs and CV of all microfluidic preparations are superior to bulk prepared control microparticles.

3.7 Figures

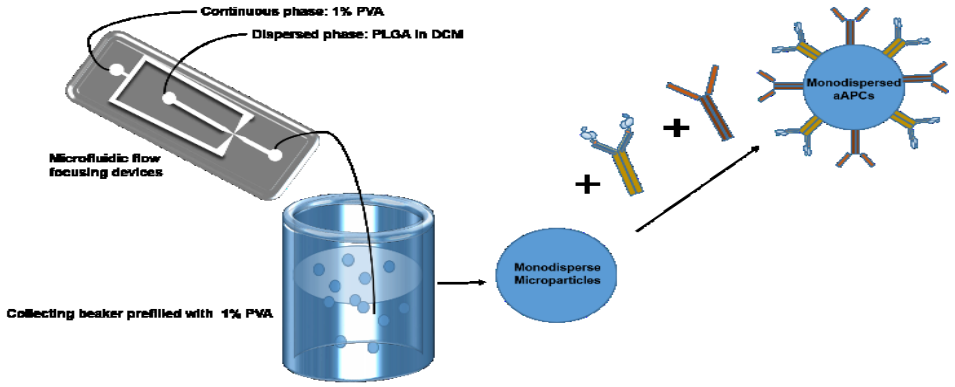

Fig. 3.1. Schematic of the microfluidic flow focusing device set up and fabrication of monodisperse artificial antigen presenting cells.

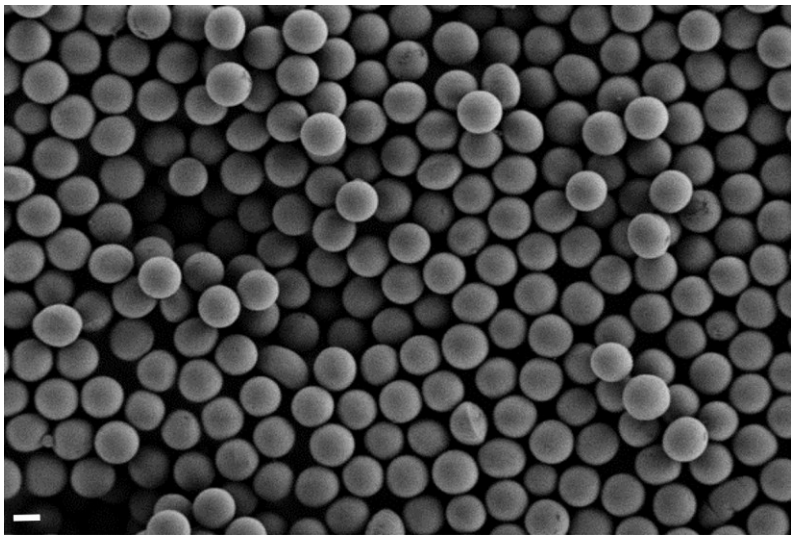

Fig. 3.2. SEM image of PLGA microparticles fabricated with dichloromethane. The monodisperse microparticles are fabricated by microfluidic flow focusing devices with dichloromethane as the polymer solvent and are of similar size and have spherical morphology by SEM imaging. Scale bar = 20 μm.

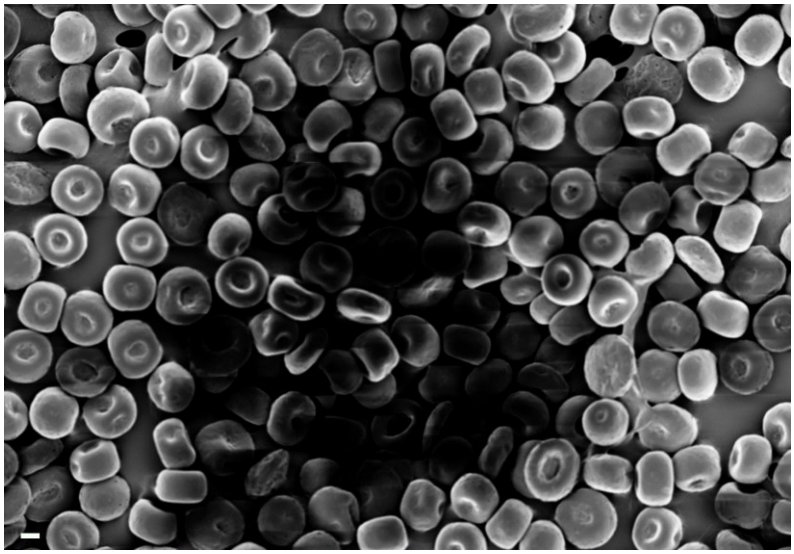

Fig. 3.3. SEM image of PLGA microparticles fabricated with ethyl acetate. The monodisperse microparticles fabricated by microfluidic flow focusing devices with ethyl acetate as the polymer solvent are of similar sizes but have “dimple” morphology as seen in SEM imaging. Scale bar = 20 μm.

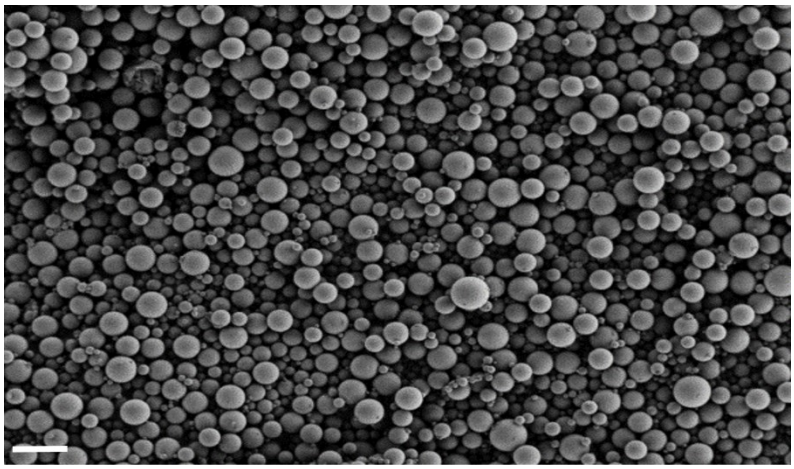

Fig. 3.4. SEM image of PLGA microparticles prepared by bulk emulsion. The microparticles fabricated by bulk emulsion with dichloromethane as the polymer solvent are polydisperse and have spherical morphology. Scale bar = 20 μm.

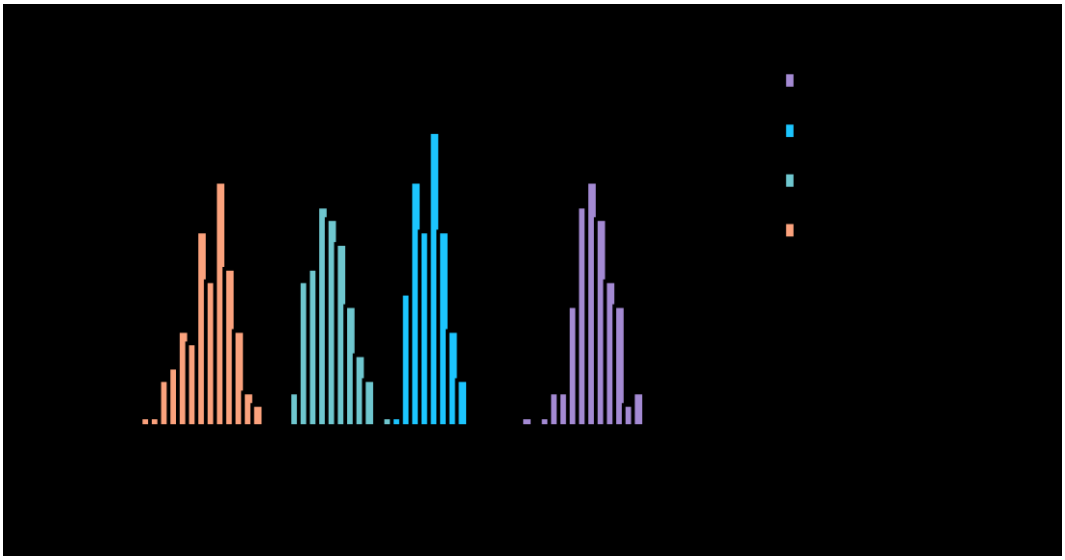

Fig. 3.5. Size distribution of PLGA microparticles as a function of polymer concentration. As the polymer concentration decreases from 20 mg/mL to 2 mg/mL, the sizes of the microparticles decrease from approximately 50 μm to 20 μm. All microparticles fabricated by MFFDs have a narrow size distribution relative to their mean size, unlike microparticles fabricated by bulk emulsion.

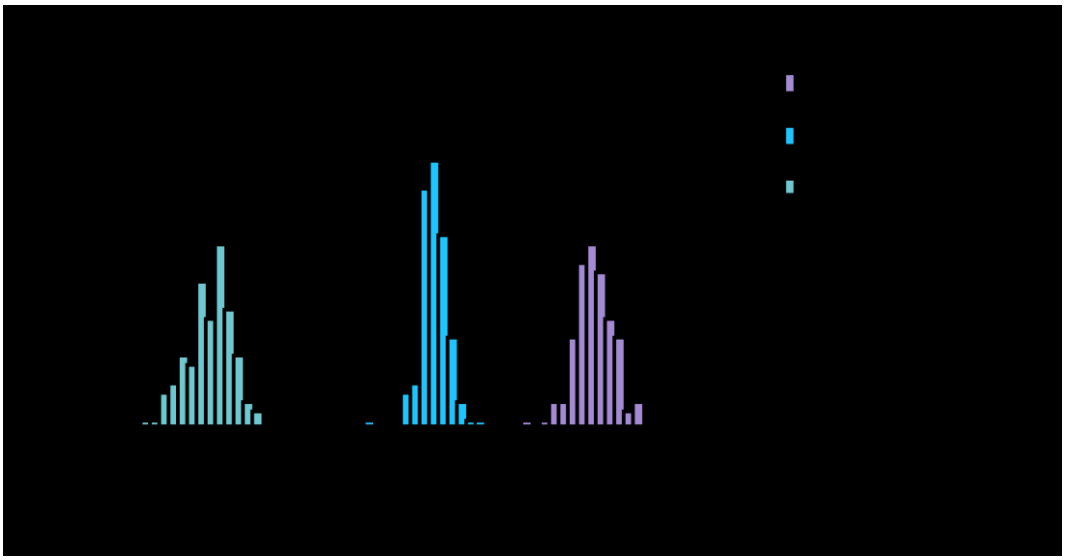

Fig. 3.6. Size distribution of large PLGA microparticles as a function of channel size. When the parameters were chose to generate larger particles (PLGA concentration was 20 mg/mL, flow rate of continuous phase is 10 mL/hr and flow rate of dispersed phase is 1 mL/hr), as the channel size of microfluidic flow focusing devices decreases, the sizes of larger microparticles decrease from approximately 50 μm to 30 μm. All microparticles made by MFFDs are monodisperse compared with microparticles made by bulk emulsion.

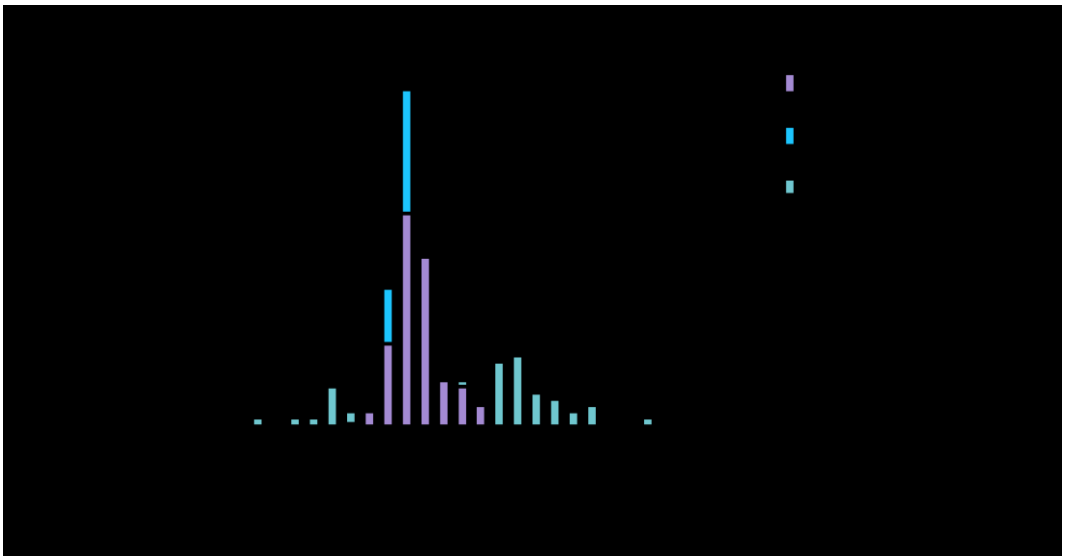

Fig. 3.7. Size distribution of small PLGA microparticles as a function of channel size. When the parameters were chose to generate smaller particles (PLGA concentration was 2 mg/mL, flow rate of continuous phase is 15 mL/hr and flow rate of dispersed phase is 0.5 mL/hr), the sizes of smaller microparticles is not affected by channel size of microfluidic flow focusing devices. All microparticles made by MFFDs are monodisperse compared with microparticles made by bulk emulsion.

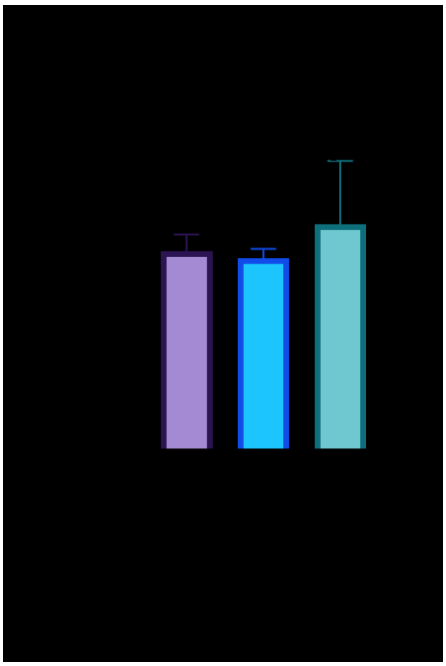

Fig. 3.8. Size of different microparticles. When the parameters were chose to generate smaller particles (PLGA concentration was 2 mg/mL, flow rate of continuous phase is 15 mL/hr and flow rate of dispersed phase is 0.5 mL/hr), as the channel size of microfluidic flow focusing devices decreases, the mean size of smaller microparticles does not change significantly.

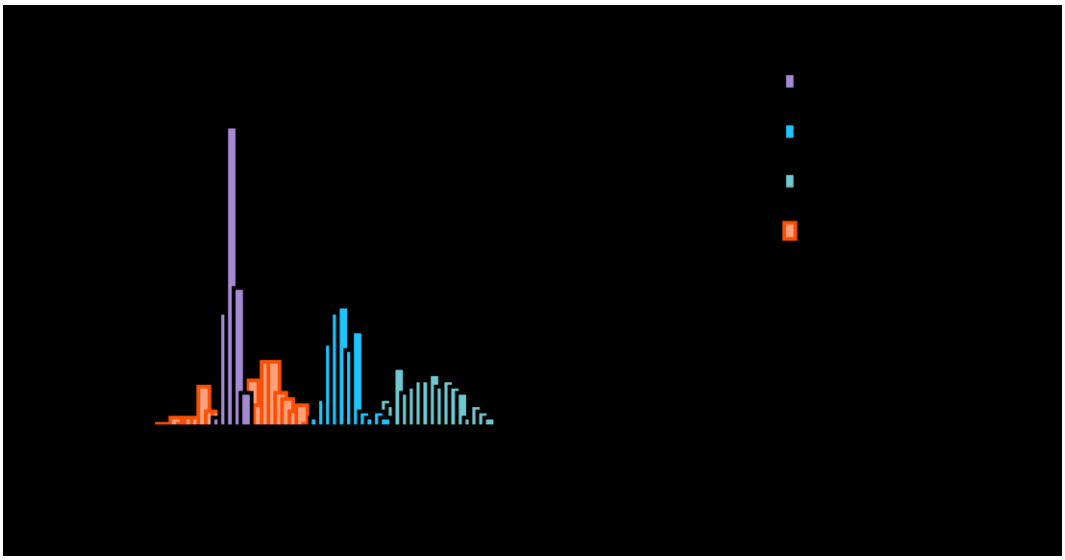

Fig. 3.9. Size distribution of PLGA microparticles as a function of flow rate. When the flow rate of the dispersed phase is maintained at 0.5 mL/hr, as flow rate of the continuous phase increases, the size of microparticles decreases. All microparticles made by MFFDs have a narrow monodisperse size distribution compared with microparticles made by bulk emulsion.

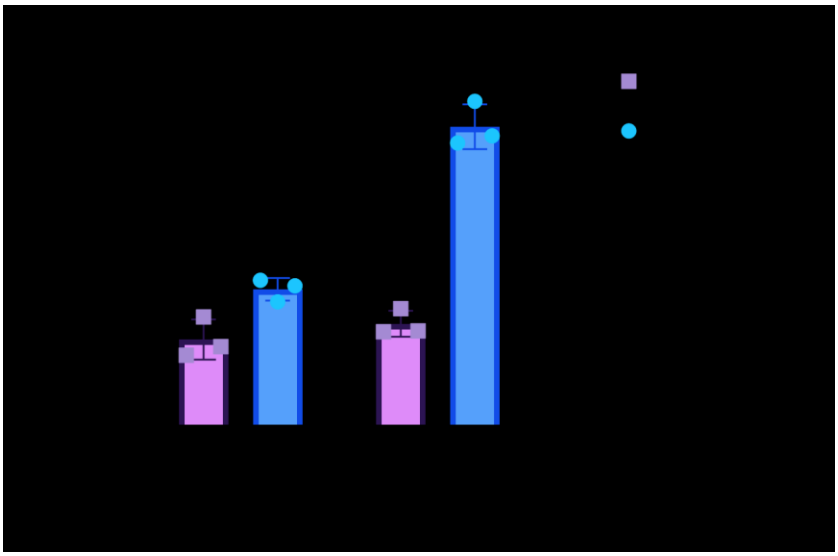

Fig. 3.10. Protein conjugation by EDC-NHS chemistry with standard conditions. By EDC-NHS chemistry, we obtain a relatively low amount of proteins conjugated on the surface of PLGA microparticles. There is also more anti-CD3 protein conjugated on the particles than anti-CD28 protein. Low dose refers to using 4 μg anti-CD3 and 5 μg anti-CD28 per mg particles. High dose refers to using 8 μg anti-CD3 and 10 μg anti-CD28 per mg particles.

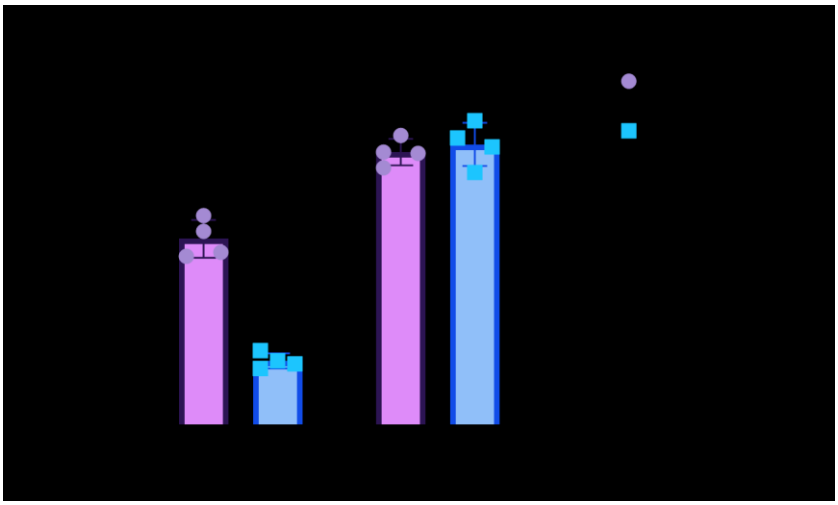

Fig. 3.11. Protein conjugation by EDC-NHS chemistry with enhanced conditions. By pre-degradation of the particle surface and sequential addition of anti-CD28 protein first and then anti-CD3 protein during conjugation, improved protein conjugation was achieved with higher amount of proteins on the surface and a balanced molar ratio of the two proteins (n=4).

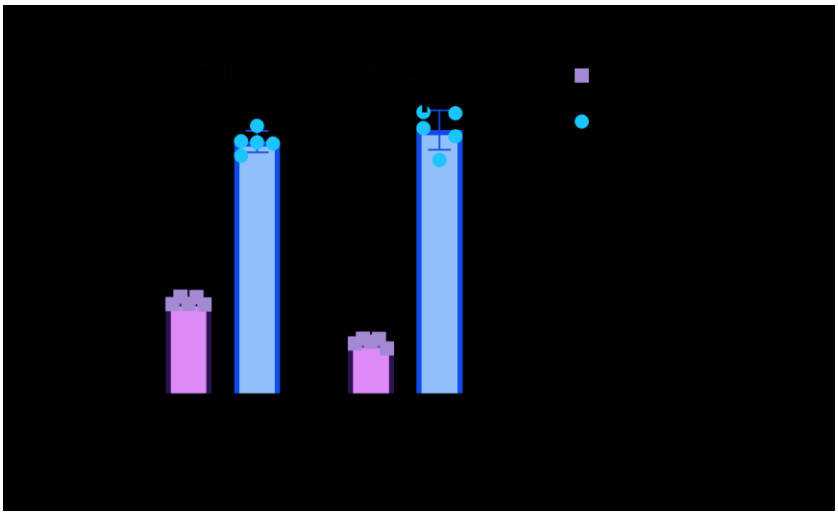

Fig. 3.12. Protein conjugation by EDC-NHS chemistry. By modified EDC-NHS chemistry, monodisperse PLGA microparticles made by MFFDs have higher conjugation efficiency than bulk emulsion PLGA microparticles for both of the proteins (n=5).

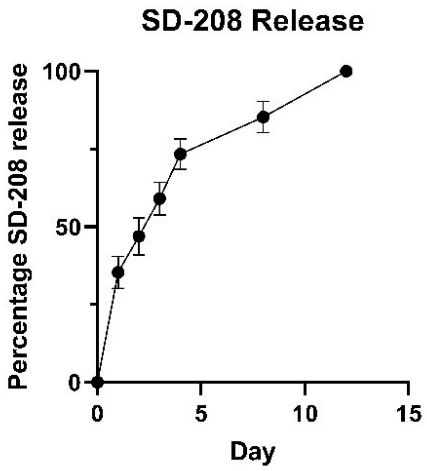

Fig. 3.13. Release profile of SD-208 from PLGA microparticles fabricated by a microfluidic device.

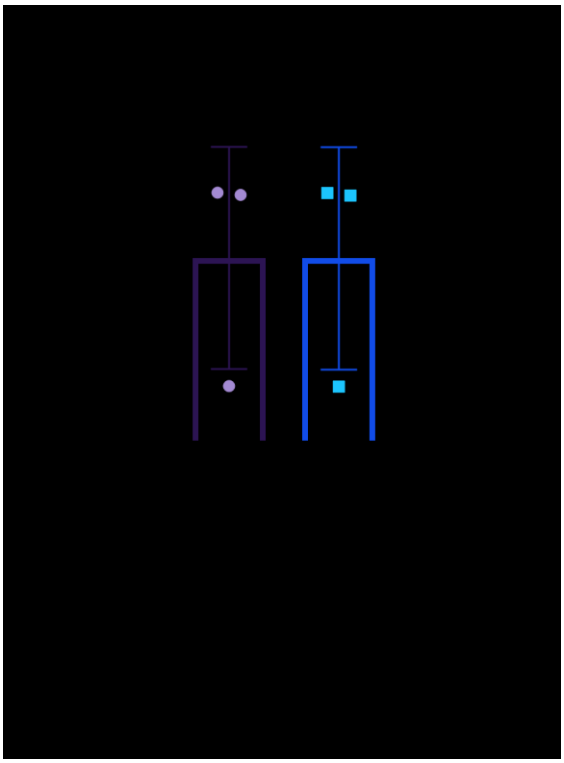

Fig. 3.14. Drug loading and encapsulation efficiency of SD-208 into monodisperse PLGA microparticles by a microfluidic device.

Chapter 4

Microfluidic emulsions of PLGA/PBAE polymer blends

4.1 Introduction

Microfluidic flow focusing devices described above are ideally used to generate single emulsion polymeric microparticles with high uniformity in size[1]. Single emulsions enable the formation of oil-in-water (O/W) and encapsulation of hydrophobic drugs in the particles. To deliver other hydrophilic payloads like peptides, proteins, and nucleic acids, a modified emulsification procedure called double emulsion (water-in-oil-in-water, (W/O/W)) is needed[2]. The application of microfluidic flow focusing devices (MFFDs) with our design could be extended to perform a W/O emulsion and a W/O/W double emulsion. A W/O first step followed by the O/W emulsion step previously described could enable the fabrication of monodisperse double emulsion polymeric microparticles and would broaden the utility of MFFDs.

In the construction of aAPCs, poly(lactic-co-glycolic acid) (PLGA) microparticles demonstrated lower than desired protein conjugation efficiency in the previously discussed experiments and new materials, such as polymer blends, could potentially improve protein conjugation. Poly(β-amino acid)s (PBAEs) are a class of cationic polymers that are used

by researchers as gene delivery vectors[3] or protein delivery vehicles[4]. PBAEs are particularly advantageous for therapeutic use because they are biodegradable via hydrolysis of their ester linkages. PLGA-PBAE blend particles showed high efficiency in protein and nucleic acid delivery[5] while maintaining the capacity of PLGA particles to slowly degrade and controllably release loaded drugs[6]. However, the ability of microfluidic flow focusing devices (MFFDs) to fabricate PLGA-PBAE microparticles and engineer control over particle size has not been previously investigated. Fabrication of scalable monodisperse PLGA-PBAE microparticles of defined size could enable enhanced delivery properties and facilitate the evaluation of other blended microparticles with well-defined physical properties.

In this chapter, we investigated the potential of MFFDs to fabricate monodisperse W/O emulsion droplets, monodisperse PLGA-PBAE blend microparticles, and functionalization of PLGA-PBAE particles into enhanced artificial antigen presenting cells (aAPCs). Our objective in this research is to broaden the application of MFFDs and to show the potential of MFFDs to be versatile platforms for particle synthesis using varied biomaterials.

4.2 Materials and Methods

Fabrications of microfluidic devices: The fabrication of microfluidic channels for PLGA-PBAE microparticle synthesis was the same as described in the methods for microfluidic device fabrication in Chapter 3. To fabricate microfluidic channels for W/O emulsion, we

bound polydimethylsiloxane (PDMS) molds on PDMS flat sheets after plasma-oxidizing the surfaces directly and without pretreatment of PVA.

Generation of water droplets in oil (W/O): The physical microfluidic device setup was the same as used to fabricate PLGA microparticles as described in Chapter 3. Instead of using PLGA in DCM as the dispersed phase and a PVA solution as continuous phase (for O/W in Chapter 3), we used 10% PVA solution as the dispersed phase and DCM as the continuous phase. To avoid aggregation of droplets, the generated droplets were collected in a beaker containing the continuous oil phase of DCM (5 mL) with the surfactants Span 80 (100 mg) and Tween 80 (33 mg) under magnetic stirring[7]. The droplets were imaged under optical microscopy.

Fabrication of PLGA-PBAE monodisperse microparticles using microfluidic devices: We followed the equipment set up for microparticle fabrication as described in Chapter 3. The PBAE we used was poly(1,4-butanediol diacrylate-co-4,4'-trimethylenedepiperidine) (B4-SP). The synthesis of B4-SP polymer by Michael addition was performed as described in the literature[8]. 4,4'-trimethylenedipiperidine (SP) (Sigma Aldrich; St Louis, MO) was dissolved in THF at 500 mg/mL and added to neat 1,4-butanediol diacrylate (B4) (Sigma Aldrich; St Louis, MO) at a 1.05:1 molar ratio (B4:SP). The mixture was stirred 2 days at 50°C. Synthesized polymer was stored as a solution in THF at -20°C. 75% w/w of PLGA and 25% w/w of B4-SP were mixed and dissolved in dichloromethane (DCM) at a concentration of 2 mg/mL. We used the parameters that fabricated 7-8 μm PLGA microparticles to generate PLGA-PBAE blend particles: the flow rate of the dispersed

phase and the continuous phase was 0.5 ml/hr and 15 ml/hr, respectively, and the channel size of the MFFDs was 50 μm. Droplets were collected in a 250 mL beaker prefilled with 50 mL of continuous phase solution on a stir plate. The generated droplets were kept in the beaker overnight to let the dispersed phase solvent evaporate. The particles were then washed three times with deionized water at 3,200 g for 5 minutes, frozen and lyophilized.

Protein conjugation: To compare the difference between monodisperse PLGA particles and PLGA-PBAE blend microparticles for protein conjugation, the same EDC-NHS conjugation procedures with pre-degradation and non-simultaneous feeding of two proteins, as described in Chapter 3, were used.

Characterization of microparticles: Microparticles were imaged under scanning electron microscopy (SEM) using a LEO/Zeiss Field-emission SEM. The sizes of microparticles were quantified manually using ImageJ[9].

Statistics: All experiments were performed with n = 5 replicates unless otherwise stated. Bar graphs indicate mean ± standard error of the mean. n.s. (not significant) indicates $p > 0.05$, * indicates $p \leqslant 0.05$, ** indicates $p \leqslant 0.01$, *** indicates $p \leqslant 0.001$, and **** indicates $p \leqslant 0.0001$. All statistics were completed using statistical analysis software modules in GraphPad Prism 8 (GraphPad Software, Inc.; La Jolla, CA). For particle size measurements, a Student's t-test was used to assess the difference between the particle sizes of PLGA microparticles and PLGA-PBAE microparticles. A Student's t-test was used to evaluate the difference in protein conjugation between PLGA microparticles and PLGA-

PBAE microparticles as well. In all cases, differences were considered significant if the p-value of the test was less than 0.05.

4.3 Results

4.3.1 Water in oil emulsion through microfluidic flow focusing devices

The microfluidic emulsions discussed in Chapter 3 using MFFDs were based on a single emulsion method, which limited the application of the fabricated monodisperse microparticles to the delivery of hydrophobic payloads that can be co-dissolved in the dispersed solvent phase. To broaden the application of the microfluidic flow focusing devices to deliver hydrophilic payloads such as proteins, we studied the application of MFFD to W/O emulsions. By enabling W/O emulsions, multiple devices could also be connected in series such that the first step, water droplets in oil (W/O), could then feed into the second step from Chapter 3 (O/W), to construct double emulsion microparticles (W/O/W) with excellent monodispersity.

To investigate the capacity of MFFDs to produce water-in-oil droplets as the first step of double emulsion, we used 10% PVA solution as the dispersed phase and dichloromethane with Span 80 and Tween 80 as surfactants to prevent aggregation as the continuous phase in the MFFDs. The microfluidic device parameters were set to 5 mL/hr and 20 mL/hr for the dispersed phase and the continuous phase, respectively. Optical microscopy was used to image the generated water droplets, and sizes and polydispersity of micro-droplets were quantified. Using the above parameters, we successfully generated 100 μm water droplets and the polydispersity remained low with a CV of 9% (**Figure 4.1**).

4.3.2 Monodisperse PLGA-PBAE blend microparticles

As the initial EDC-NHS chemistry had a low conjugation efficiency for the PLGA microparticles, and recent work shows that poly-(beta-amino)-ester (PBAE)-PLGA blend polymeric particles can have improved *in vivo* efficacy for protein presentation[10], we investigated a 75% PLGA and 25% PBAE blend. The polymers were first dissolved in DCM as the dispersed phase in MFFDs to produce PLGA-PBAE blended monodisperse microparticles. The microfluidic device parameters were set to be the same as the production of monodisperse artificial antigen presenting cells described in Chapter 3. The monodisperse PLGA-PBAE microparticles were imaged via SEM, and the sizes and monodispersity were quantified by manual image analysis. There was not any significant difference between the sizes and monodispersity of PLGA-PBAE blend microparticles and PLGA microparticles (**Figure 4.2 and Figure 4.3**), which indicated that the devices were versatile to be used in the synthesis of monodisperse microparticles of different material composition and by opposite processing (O/W vs/ W/O) to achieve the same reproducible robust results. Monodisperse PLGA-PBAE blend microparticles showed an improved protein conjugation via EDC-NHS conjugation compared to bulk-prepared PLGA particles (**Figure 4.4**). Both microparticle types were made into aAPCs by following the same procedure that was previously optimized for PLGA aAPCs as discussed in Chapter 3. Namely, anti-CD28 protein conjugation was performed first for 3 hrs, followed by anti-CD3 conjugation. While this sequential treatment was required for construction of PLGA aAPCs, it does not look like it is necessary for construction of PLGA-PBAE aAPCs. This

is because with PLGA-PBAE aAPCs, significantly more anti-CD28 antibodies conjugated to the surface of the PLGA-PBAE microparticles following the sequential addition protocol. A likely interpretation is that for cationic PBAE polymer, anionic protein can non-specifically absorb preferentially to the surface[4], and the anti-CD28 antibodies that were added first were readily absorbed by the PBAE surface first, saturating the ability of PLGA-PBAE to subsequently equitably absorb anti-CD3 proteins. This resulted in only a small portion of anti-CD3 proteins being conjugated to PLGA-PBAE microparticles. Notably, similar total protein levels on the surface of the particles were found with both the monodisperse PLGA microparticles and the monodisperse PLGA-PBAE microparticles. With further tuning of timing and feed-stock ratios, it is very likely that the monodisperse PLGA-PBAE microparticles can be fabricated with a 1:1 ratio of the two surface bound proteins just like the monodisperse PLGA microparticles.

4.4 Conclusion and Discussion

Through this study, we have broadened the application of the microfluidic devices from oil-in-water emulsions to water-in-oil emulsions, demonstrating their potential for more versatile production of monodisperse microparticles. The ability of MFFDs to fabricate PLGA-PBAE microparticles can broaden the application of the devices to gene delivery and protein delivery due to the inherent delivery characteristics of PBAEs and PLGA-PBAE blended polymers. The monodisperse PLGA-PBAE blended microparticles of defined size are promising for future investigation as artificial antigen presenting cells

and may have superior ability to bind and activate T cells compared to more conventional PLGA microparticles.

4.5 References

1. Xu, Q., et al., *Preparation of monodisperse biodegradable polymer microparticles using a microfluidic flow-focusing device for controlled drug delivery.* Small, 2009. **5**(13): p. 1575-1581.
2. Li, Y.-P., et al., *PEGylated PLGA nanoparticles as protein carriers: synthesis, preparation and biodistribution in rats.* Journal of controlled release, 2001. **71**(2): p. 203-211.
3. Green, J.J., R. Langer, and D.G. Anderson, *A combinatorial polymer library approach yields insight into nonviral gene delivery.* Accounts of chemical research, 2008. **41**(6): p. 749-759.
4. Rui, Y., et al., *Carboxylated branched poly (β-amino ester) nanoparticles enable robust cytosolic protein delivery and CRISPR-Cas9 gene editing.* Science advances, 2019. **5**(12): p. eaay3255.
5. Balashanmugam, M.V., et al., *Preparation and characterization of novel PBAE/PLGA polymer blend microparticles for DNA vaccine delivery.* The Scientific World Journal, 2014. **2014**.
6. Zhang, C., et al., *Stepwise pH-responsive nanoparticles containing charge-reversible pullulan-based shells and poly (β-amino ester)/poly (lactic-co-glycolic acid) cores as carriers of anticancer drugs for combination therapy on hepatocellular carcinoma.* Journal of Controlled Release, 2016. **226**: p. 193-204.
7. Anselmo, A.C., et al., *Elasticity of nanoparticles influences their blood circulation, phagocytosis, endocytosis, and targeting.* ACS nano, 2015. **9**(3): p. 3169-3177.

8. Li, C., et al., *(3-Aminopropyl)-4-methylpiperazine end-capped poly (1, 4-butanediol diacrylate-co-4-amino-1-butanol)-based multilayer films for gene delivery.* ACS applied materials & interfaces, 2013. **5**(13): p. 5947-5953.

9. Schneider, C.A., W.S. Rasband, and K.W. Eliceiri, *NIH Image to ImageJ: 25 years of image analysis.* Nature methods, 2012. **9**(7): p. 671-675.

10. Rhodes, K.R., et al., Biomimetic Tolerogenic Artificial Antigen Presenting Cells for Regulatory T Cell Induction. Acta Biomaterialia, 2020.

4.6 Figures

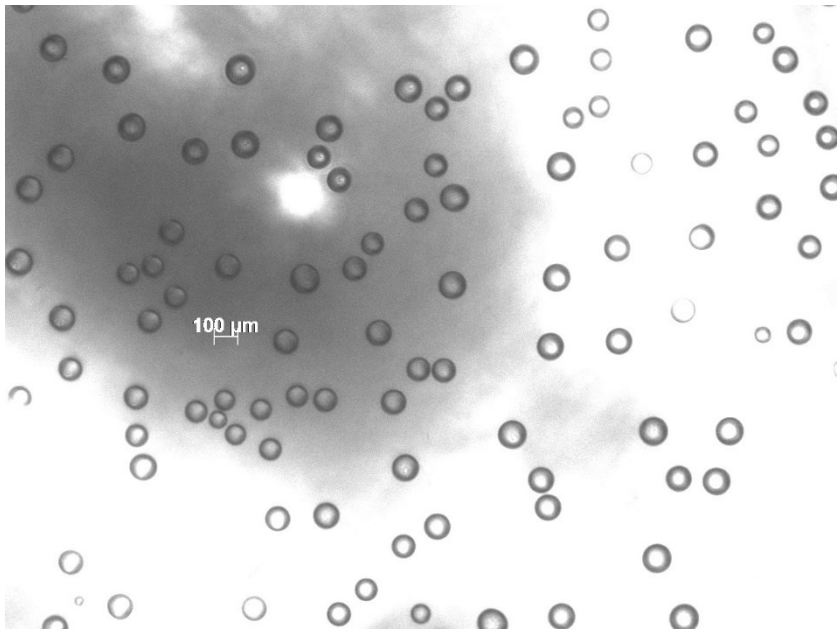

Fig. 4.1. Optical microscopy images of water droplets in a hydrophobic phase generated by microfluidic W/O emulsion. Scale bar = 100 µm.

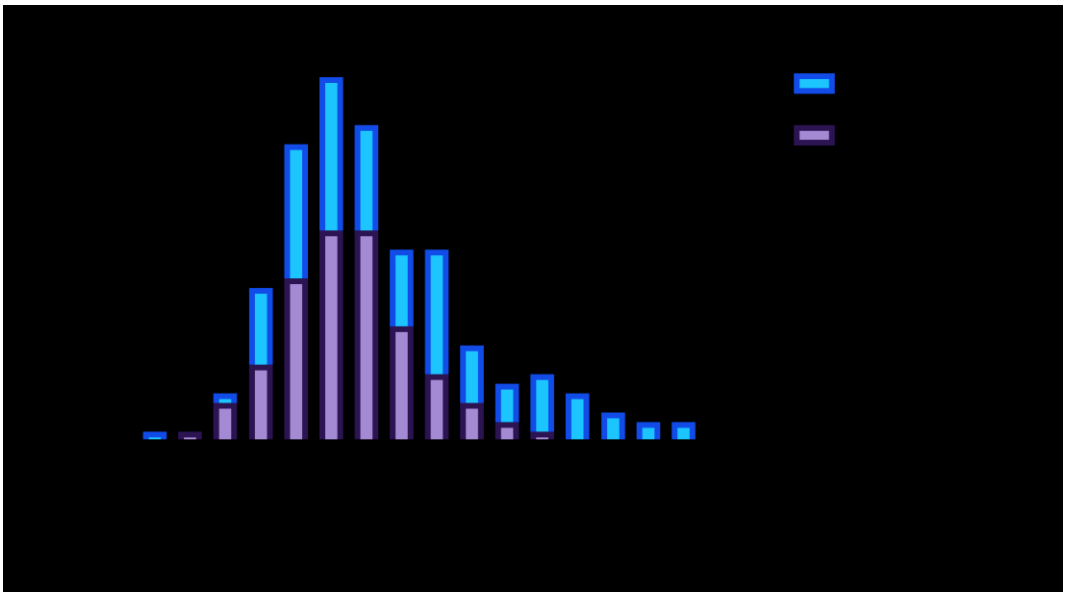

Fig. 4.2. Size distribution of different microparticles. Microparticles made of PLGA and PLGA-PBAE blends have similar size distribution characteristics and excellent monodispersity.

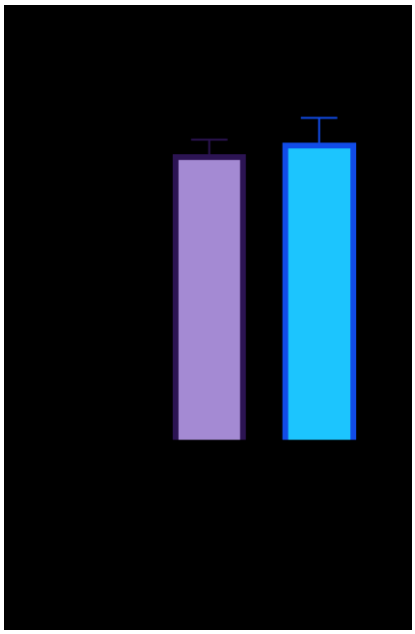

Fig. 4.3. Size of different microparticles. The sizes of microparticles does not change significantly between monodisperse PLGA microparticles and PLGA-PBAE blended microparticles both made by MFFDs.

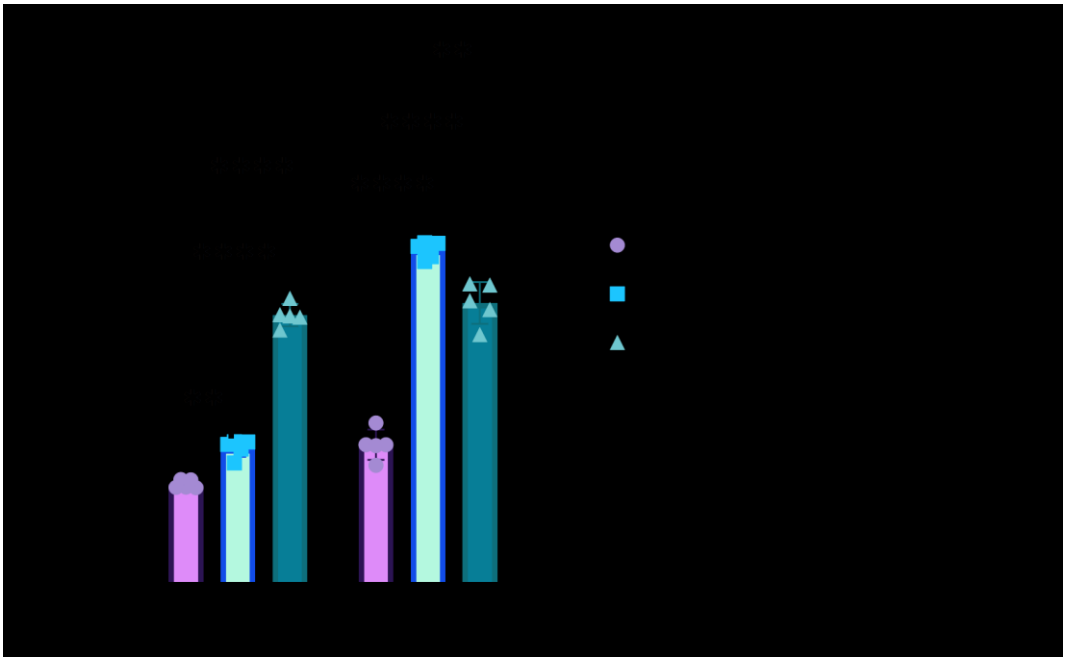

Fig. 4.4. Protein conjugation by EDC-NHS chemistry. Monodisperse microparticles made by MFFDs have higher conjugation efficiency for both of the proteins compared with microparticles made by bulk emulsion. Between the two monodisperse microparticles, there are more anti-CD28 antibodies on the PLGA-PBAE microparticles and less anti-CD3 antibodies on the PLGA-PBAE microparticles compared to the PLGA microparticles.

Chapter 5

Future Directions

5.1 Future Directions

Due to the COVID-19 pandemic, this study was halted at the stage of physical and chemical characterization of the monodisperse aAPCs. After the lab reopens, *in vitro* and *in vivo* functional tests will be conducted to examine T cell activation and proliferation by the monodisperse aAPCs.

In this work, monodisperse PLGA microparticles with tunable sizes have been successfully developed through microfluidic flow focusing devices (MFFDs), and we have successfully demonstrated that monodisperse microparticles of cell-like size have the capacity to be functionalized as artificial antigen presenting cells (aAPCs). Our monodisperse microparticles exhibit increased protein conjugation efficiency compared with microparticles made by bulk emulsion and the capacity to release loaded hydrophobic immunoregulatory drugs in a controlled fashion over time. The scalable and robust fabrication procedure, the low variability between batches, the excellent control of particle size, and the excellent monodispersity at each of these particle sizes, allows researchers the ability to better standardize the particle-based therapies including drug delivery devices and biomimetic aAPCs.

We have preliminarily shown the potential of the microfluidic devices to be a versatile particle synthesis platform for microparticles of different, payloads, materials, and processing conditions. We only just demonstrated that MFFDs can be used in W/O emulsion and O/W emulsion to generate the same type of monodisperse droplets and polymeric microparticles of the same monodisperse size. It would be interesting to explore in the future how putting these two validated devices and processes together in series could facilitate the generation of monodisperse double emulsion particles. Further, modified designs of MFFDs can be developed to do these two steps on a single chip rather than performing a traditional two-step bulk double emulsion process[1]. A microfluidic chip for double emulsion would be useful for monodispersity, reproducibility, and scalability, and also to improve efficiency and save on costs of expensive biological payloads such peptides, proteins and nucleic acids.

The ability of MFFDs to fabricate monodisperse PLGA-PBAE microparticles broadens the application of the devices to synthesize gene delivery vectors and protein delivery vehicles. The efficacy of such monodisperse microparticles for gene delivery and/or protein delivery warrants further study.

Overall, emulsions via microfluidic devices have the potential to provide a versatile technology for polymeric microparticle production and promote particle-based therapies in targeted drug delivery, immunotherapies, and gene therapies.

5.2 References

1. Bukofzer, S., et al., *Industry perspective on the medical risk of visible particles in injectable drug products.* PDA Journal of Pharmaceutical Science and Technology, 2015. **69**(1): p. 123-139.

Chapter 6

Curriculum Vitae

EDUCATION BACKGROUND

08/2018-present Department of Biomedical Engineering, The Johns Hopkins University, Baltimore, USA

Major: M.S.E. candidate in Biomedical Engineering **GPA:** 3.94/4.0

Core courses: Tissue Engineering (A) / Cellular Engineering (A-) / Cell and Tissue Engineering Lab (A) / Advanced Biomaterials (A) / Advanced Topics in Regenerative and Immune Engineering (A) / Introduction to Polymeric Materials (A)

01/2017-06/2017 Undergraduate Exchange Program, University of California-San Diego, La Jolla, USA

Major: Bioengineering **GPA:** 4.0/4.0

Core courses: Human Physiology I (A+) / Principle of Bioinstrumentation Design (A) / Elements of Materials Science (A) / MATLAB Program for Engineering Analysis (A+) / Neurobiology and Behavior (A) / Human Nutrition (A)

09/2014-06/2018 School of Life Science & Technology, Huazhong University of Science and Technology(HUST), China

Major: B.S. in Biomedical Engineering **GPA:** 3.88/4.0 **Ranked:** 3/103 (Ranked 1st in junior year)

Core courses: Biochemistry and Molecular Biology (94) / Basic Chemistry (92) / Biomaterials (93) / Introduction to Tissue Engineering (95) / Compatibility Evaluation of Biomaterials (95)

SCHOLARSHIPS & AWARDS

06/2018 Outstanding graduate, HUST

10/2017 Merit Student, HUST (Top 2%, highest scholarship for academic performance at HUST)

10/2016 Outstanding Undergraduate International Exchange Scholarship, CSC (Top 1%)

RESEARCH EXPERIENCE

10/2018-present, Graduate Research Assistant, Translational Tissue Engineering Center, Johns Hopkins University, USA

Project: Monodisperse Polymeric Microparticles as Artificial Antigen Presenting Cells for Cancer Immunotherapy

Advisor: Dr. Jordan Green, Professor in Department of Biomedical Engineering, Johns Hopkins University

- **Project Goal:** To generate monodisperse PLGA microparticles via microfluidic flow focusing devices (MFFD) as artificial antigen presenting cells to boost the immune system as cancer therapy.
- **Preliminary Results:** PLGA particles with diameters between 6 μ m to 50 μ m and low variability were made. Small molecules SD-208 (TGF-beta inhibitor) could be loaded in and released sustainably from monodisperse microparticles and anti-CD3 - anti-CD28 could be conjugated on the surface of microparticles through EDC-NHS conjugation to construct artificial antigen presenting cells (aAPCs).
- **Duties Included:** (1)Designed and fabricated MFFD devices. (2)Produced SD-208 loaded, anti-CD3, anti-CD28 conjugated, monodisperse artificial antigen presenting cells (maAPCs) and

characterized morphology, drug loading and release profile, conjugation efficiency of maAPCs.

Assisted in Projects: Biomimetic Anisotropic Polymeric Nanoparticles Coated with Natural Cell Membranes

Advisor: Dr. Jordan Green, Professor in Department of Biomedical Engineering, JHU
Elana Ben-Akiva, Ph.D. Candidate, Department of Biomedical Engineering, JHU

- **Project goal:** To generate anisotropic PLGA nanoparticles with red blood cell membrane coating for toxin removal; to generate anisotropic PLGA particles with platelet membrane coating for targeted drug delivery to metastatic cancer cells
- **Duties Included:** (1)Produced anisotropic erythrocyte membrane coated PLGA nanoparticles and platelet membrane coated PLGA particles. (2)Conducted in vitro macrophage uptake experiment. (3)Assisted in vivo biodistribution experiments.
- **Publication:**
  Biomimetic Anisotropic Polymeric Nanoparticles Coated with Red Blood Cell Membranes for Enhanced Circulation and Toxin Removal, Elana Ben-Akiva, Randall A. Meyer, **Hongzhe Yu**, Jonathan T. Smith, Drew M. Pardoll, Jordan J. Green, Science Advances, *Science Advances, 6(16), eaay9035.*

12/2017-5/2018, Advanced Biomaterials and Tissue Engineering Research Center, HUST, China
Undergraduate Thesis: Impact of materials stiffness on stem cell differentiation
Advisor: Dr. Shengmin Zhang, Professor in Department of Biomedical Engineering, HUST

- **Project goal:** To study the impact of polyacrylamide hydrogel stiffness on rat bone-marrow-derived stem cells differentiation
- **Duties Included:** (1)Produced and characterized polyacrylamide hydrogel substrates of different stiffness. (2)Cultured rat's bone-marrow-derived mesenchymal stem cells on produced polyacrylamide hydrogel substrates. (3)Conducted immunofluorescence experiment and histological strain on cultured rBMSCs to examine the direction of differentiation.

04/2017-08/2017, Undergraduate Research Assistant, S.Leutgeb's Lab, UC San Diego, USA
Project: Effects of Shifting Endogenous Theta Frequency on Spatial Representations in Medial Entorhinal Cortex
Advisor: Dr. Stefan Leutgeb, Professor in Division of Biological Science, UCSD
Dr. Clare Quirk, Department of Biological Science, UCSD

- **Project goal:** To study on whether removing the speed modulation of theta decrease the precision of mEC special cells or disrupt the special periodicity of grid cells
- **Duties included:** (1)Built microdrives and optic fibers as parts of chronic implants to apply optical ontogenetic stimulation and record local field potential in medial septal area. (2)Assisted with behavioral tests on mice and performed histology on the brain. (3)Analyzed data such as mean gridness score and firing rate between no stimulation and stimulation recordings.

EXTRACURRICULAR ACTIVITIES

Invited outstanding technology entrepreneurs in Wuhan for speeches and organized semiannually Youth to Business Forum as department head of Human Resources of AIESEC HUST 03/2015-06/2016

Volunteered in the 2nd China College Students' Innovation and Entrepreneurship Competition, and won the title of *Outstanding Volunteer* (100 out of over 1000 volunteers) 09/2016-10-2016

COMPUTER AND LAB SKILLS

C, MATLAB, Verilog HDL, EDA software (cadence), CAD, Clean room, Rodent surgery, Cell culture, Scan Electron Microscopy, Confocal Fluorescent Microscopy, Flow cytometry